PHOTOELECTROCHEMICALLY INITIATED POLYMERIZATIONS

by

Grant H. Fritzke

B.Sc., Trinity Western College, 1982.

A THESIS SUBMITTED IN PARTIAL FULFILLMENT OF

THE REQUIREMENTS FOR THE DEGREE OF

MASTER OF SCIENCE

in the Department

of

Chemistry

SIMON FRASER UNIVERSITY

November, 1986

APPROVAL

Name: Grant H. Fritzke

Degree: Master of Science

Title of Thesis: Photoelectrochemically Initiated Polymerizations

Examining Committe:

Chairman: Dr. F.W.B. Einstein

Dr. B.L. Funt
Senior Supervisor

Dr. S.R. Morrison

Dr. P. W. Percival

Dr. A.G. Sherwood

Date Approved: Feb 6, 1987

PARTIAL COPYRIGHT LICENSE

I hereby grant to Simon Fraser University the right to lend my thesis, project or extended essay (the title of which is shown below) to users of the Simon Fraser University Library, and to make partial or single copies only for such users or in response to a request from the library of any other university, or other educational institution, on its own behalf or for one of its users. I further agree that permission for multiple copying of this work for scholarly purposes may be granted by me or the Dean of Graduate Studies. It is understood that copying or publication of this work for financial gain shall not be allowed without my written permission.

Title of Thesis/Project/Extended Essay

Photoelectrochemically Initiated Polymerizations

Author:

(signature)

Grant H. Fritzke

(name)

March 2 1987

(date)

ABSTRACT

Photoelectrochemically initiated polymerizations were investigated using n-type titanium dioxide single crystal electrodes as photoanodes. Polymerizations were initiated in the anode compartment of a divided photoelectrochemical cell by the passage of a photoinduced current. A 200 watt high pressure mercury lamp was used as an illumination source.

Acrylamide was polymerized in aqueous solution using various supporting electrolyte systems: sulfuric acid, sodium sulfate, tetraethylammonium perchlorate and acetic acid - sodium acetate. Current efficiencies, ie. the moles of monomer polymerized per faraday passed, for the first three electrolyte systems studied were comparable. A 50 fold increase in current efficiency was noted for the acetic acid - sodium acetate system. The reaction mechanism was established to be free radical.

The photoinduced current increased linearly with the intensity of incident light within the range of intensities used. Rates of initiation and polymerization as well as polymer yields and molecular weights for acrylamide were controlled by the intensity of light focussed on the semiconductor electrode. A typical polymerization rate was 6.7×10^{-5} moles/litre-sec. Molecular weights showed an inverse half-power dependence on the relevant photocurrent.

The photoelectrochemical polymerization of solutions of isobutyl vinyl ether and of ethyl vinyl ether in acetonitrile

with a tetraethylammonium perchlorate supporting electrolyte resulted in formation of oligomers. Low molecular weight polymers of isobutyl vinyl ether were produced via photoelectrochemical initiation in solutions of dichloromethane using a tetrabutylammonium perchlorate supporting electrolyte. Initiation mechanisms for the cationic polymerizations of the vinyl ethers are proposed.

TO PAT

ACKNOWLEDGEMENTS

I wish to offer my thanks to Dr. B. L. Funt for his supervision throughout the course of this work.

I also wish to thank Dr. P. M. Hoang, Messrs. S. V. Lowen, S. Holdcroft, F. Orfino and E. Peters for their stimulating comments and discussions.

Thanks are also due to Mrs. N. Hykaway for preparing the semiconductor material.

Last, I would like to express my appreciation to Mr. I. W. Rutherford for the printing of the thesis.

TABLE OF CONTENTS

LIST OF TABLES

LIST OF FIGURES

I. INTRODUCTION

I.1. General Aspects Of Polymers

A polymer is a large molecule built up by the repetition of small, chemical units. In some cases, the repeated addition of units is linear, much as a chain is built up from its links. In other cases, the chains are branched or interconnected to form three-dimensional networks. The repeat unit of the polymer is usually equivalent or nearly equivalent to the monomer, or starting materials from which the polymer is formed. The length of the polymer chain is specified by the number of repeat units in the chain. This is called the degree of polymerization. The molecular weight of the polymer then, is the product of the degree of polymerization and the molecular weight of the repeat unit. The length of a chain is determined by various events in the polymerization reaction. Since typical polymers consist of mixtures of many molecular species, molecular weight methods only yield average values. Several different averages are important and have become standards by which molecular weights are reported. In general, two averages are most significant, number average (M_n) and weight average (M_w) molecular weights. The former average is defined as the total weight of the polymer divided by the number of moles which it contains. M_n is a measure of the number of molecules present with no regard to size. The

number average value can be written

$$M_n = \frac{\sum_i N_i M_i}{\sum_i N_i} \qquad [1]$$

where N_i is the number of i^{th} species and M_i is the molecular weight of the i^{th} species. The weight average molecular weight depends not only on the number of units within a chain but also on the weight of the molecule. This can be written

$$M_w = \frac{\sum_i N_i M_i^2}{\sum_i N_i M_i} \qquad [2]$$

where the symbols have the equivalent association as before. The molecular weight distribution, which is a measure of the range of lengths of the chains, is often measured by the ratio of

$$\text{Distribution} = M_w/M_n \qquad [3]$$

Viscosity measurements of a polymer solution give a measure of the size of the polymer, and may be empirically related to the molecular weight of a linear polymer by the Mark-Houwink equation

$$[n] = KM^a \qquad [4]$$

where k and a are empirical constants dependent on the nature of

the polymer, the solvent and temperature, M the molecular weight and [n] the intrinsic viscosity. Intrinsic viscosity, [n], is defined as specific viscosity, n_{sp}, divided by the concentration of polymer in solution, c, in the limit where c approaches zero.

$$[n] = \lim_{c \to 0} \frac{n_{sp}}{c} \qquad [5]$$

Gel permeation chromatography (GPC), is a powerful technique for separating polymer molecules according to size using chromatographic columns filled with beads of a rigid porous gel or porous glass. When a sample of dilute polymer solution is introduced into a solvent stream flowing through the column, the dissolved polymer molecules flow past the porous beads. As the solvent stream carries the polymer molecules past the beads, the molecules can diffuse into the internal porous structure of the beads to an extent dependent upon the size of the molecule and the pore size distribution of the beads. The larger molecules enter only a small fraction of the internal area of the beads or are totally excluded. The shorter length molecules penetrate the pores of the beads to a greater extent. As a result, the larger a molecule is the less time it spends inside the columns and the quicker it is eluted. The different molecular species are eluted from the column in order of their molecular size as

distinguished by their molecular weight, the largest emerging first. Both number average and weight average molecular weight as well as molecular weight distribution of a polymer sample can be determined from the chromatograph.

As the primary cohesive forces between molecules are intermolecular forces of attraction, many physical properties of polymers, such as volatility, viscosity, surface tension and frictional properties, and miscibility are greatly influenced by increasing molecular weights. The high molecular weights of polymers allows these forces to build up enough to impart excellent strength, dimensional stability, elasticity, and other mechanical properties to the substances.

I.2. Types of Polymerizations

It is convenient to classify polymers according to the type of reactions involved in their synthesis. Polymerizations can be separated into two main categories according to the type of reaction by which the polymer was formed, a) condensation reactions, and b) addition reactions.

Condensation polymerization is a method of polymerizing molecules which contain at least two functional groups. The polymers are formed from bi or poly functional monomers with the elimination of a byproduct in a stepwise intermolecular manner. Polymerization continues until almost all of one reagent is consumed.

Addition polymerization is a chain mechanism which involve active centers on the end of a growing polymer chain. The active

centers may be either free radical, anionic or cationic in nature. The steps of addition polymerization can schematically be described as follows

a) Initiation: the formation of active centers.

$$\text{Initiator} \longrightarrow R' \qquad [6]$$

$$R' + M \longrightarrow R^* \qquad [7]$$

b) Propagation: the addition of monomer to the active site of the chain.

$$R_n^* + M \longrightarrow R_{n+1}^* \qquad [8]$$

c) Chain transfer: The transfer of the active site to another molecule, producing a termination of the growing chain and an active species capable of initiating another chain.

$$R_n^* + S \longrightarrow P_n + S^* \qquad [9]$$

d) Termination: Destruction of the active center.

$$R_n^* \longrightarrow P_n \qquad [10]$$

In the above equations, M represents a monomer unit, R' the initiating species, R_n^* a propagating chain with a degree of polymerization n, S the chain transfer agent and P_n the inactive polymer.

I.3. Chemical Initiators for Chain Polymerization

In common with other chain reactions, addition polymerizations are initiated by reactive species or intermediates, such as free radicals, carbonium ions, carbanions and charge transfer complexes. To initiate a reaction, reactive species may be generated in situ by a suitable chemical process. Such processes include the formation of radicals by thermal decomposition of peroxides, generation of anion and cation radicals by way of electron transfer between two molecules, and many other reactions. Table I summarizes the types of reagents which can initiate addition polymerization of vinyl compounds.

I.4. Physical Initiation Techniques

The use of chemical catalysts and initiators provides only one method for the induction of chain polymerization. Initiation energy required for polymerization can also be supplied thermally, through irradiation with high-energy or ionizing radiation, with visible or ultraviolet light or by an electrolytic process. In general, the conversion of monomer to polymer will occur through the normal propagation, termination and transfer reactions while the initiation process is greatly affected by the technique used to initiate polymerization.

I.4.1. High-Energy Radiation

Chain polymerizations can be induced by irradiation of the monomer with high-energy radiation, such as x-rays, γ-rays, α-particles, high-energy electrons and protons (1,2). Polymerization of the monomer can be performed in the bulk phase or in solution. The absorption of energy by the monomer is far less selective when ionizing radiation is used than for most other initiating techniques. All species in the system (monomer and solvent) can absorb energy and decompose to yield free radicals. The radicals then initiate polymerization.

I.4.2. Photoinitiation

The energy required to initiate polymerization may be introduced to the system by absorption of a photon (3-6). Photochemical or photoinitiated polymerizations occur when radicals are produced by ultraviolet and visible light irradiation of a reaction system. In general, the absorption of a photon results in initiation by one of two pathways:

a) A species within the system absorbs the photon, and proceeds to decompose into radicals which act as polymerization initiators.

b) A species undergoes excitation through absorption of a photon and the excited species interacts with a second compound. This is

Table I

Types of chemical initiators for chain polymerization

Initiator type	Formula or example
a) Organic or hydro-peroxides	Benzoyl peroxide 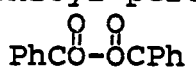
b) Redox agents	Persulfates with reducing agents, Hydroperoxides and ferrous ions
c) Azo compounds	Azobisisobutyronitrile 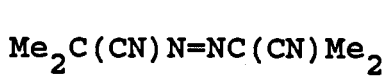
d) Alkali metal suspensions	Sodium in tetrahydrofuran or ammonia
e) Alkyl or aryllithium reagents	
f) Organic anion radicals	Sodium naphthalenide
g) Ziegler-Natta catalysts	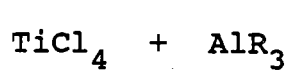
h) Strong acids	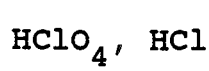
i) Lewis acids	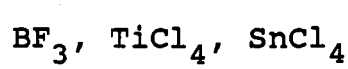

followed by either energy or electron transfer, by way of a redox reaction, to a second compound to form radicals derived from the latter and/or former compound(s).

Any monomer that will undergo chain polymerization is susceptible to photopolymerization. The absorption of light simply produces free radicals or ions by providing the energy necessary to effect decomposition. Unfortunately, only a few unsaturated monomers are known which absorb light between 250 and 500 nm, the most convenient range of wavelength for practical use. For other monomers, a photosensitizer must be added to the system. Photosensitizers are compounds which absorb light in a convenient region of the spectrum and then transfer the energy, to the monomer or dissociate into free radicals. Several significant practical advantages can be taken advantage of using a photoinitiation process. Radical production and polymerization can be spatially directed and turned on and off simply by turning the light source on and off. Additionally, initiation rates can be controlled by a combination of the source of radicals, light intensity and temperature.

I.4.3. Electrochemical Initiation

The application of an external source of energy, in the form of electrical energy, provides another means of furnishing the energy required to activate a reaction. Therefore, electrochemically initiated reactions bear a close similarity to photolytic reactions whose external energy source is light. In

each instance, a new dimension of control is presented for the polymerization process. The reaction is not solely dependent on the initial concentrations of reactants and initiator. Electrochemical initiation is controlled through two parameters, potential and current. In a given system, the reactions that occur at an electrode depend on the potential of the electrode. The potential applied to the working electrode establishes the energy of the electronic species which reacts with substrates in solution. The reaction which occurs at the electrode will be either the oxidation of a species to produce radicals or cation radicals or the reduction of a species to produce radicals or anion radicals. The second parameter, current, is a measure of the rate at which the reaction occurs. By controlling the current during polymerization, it is possible to program the course of a reaction to follow a certain rate. When the reaction rate determines the molecular weight of the polymer, it is possible to control the properties of the final polymer. Several excellent reviews covering the field of electrochemical initiation are available (7-12).

I.5. Photoelectrochemical Applications for Polymerization

I.5.1. Introduction

The recent interest in photoelectrochemical processes for the production of potential fuels was pioneered in 1970 by Fujishima and Honda (13) who reported the sustained oxidation of water at illuminated n-TiO_2 in a photoelectrochemical cell. Although the related reduction of hydrogen at the counter

electrode could not be accomplished without the application of a 0.2 volt external bias, their paper unleashed a world wide effort at discovering new, alternative routes for catalyzed photo-redox reactions occurring on illuminated semiconductors. The conceptual model of using semiconductor/liquid junctions as sites for light induced redox reactions has been used as the basis for research in the areas of efficient hydrogen generation by water splitting (14-18), the Photo-Kolbe synthesis to produce saturated alkanes from carboxylic acids (19-22) and other synthetic uses such as the photocatalytic synthesis of ammonia from water and nitrogen, (23) the photocatalytic formylation of primary and secondary amines (24), and the photoelectrochemical oxidation of propylene to propylene oxide (25). The intense investigation of photoelectrochemical events over the past 16 years has resulted in the appearance of many reviews covering the field (26-33).

I.5.2. Basic Principles

Semiconductors are characterized by an energy gap between two existing ranges of energy states for electrons. The lower energy level is the valence band (VB) containing the bonding electronic states which are occupied. The high energy level is the conduction band (CB) consisting of non-bonding or anti-bonding energy states which are normally unoccupied. These bands are separated by a forbidden region or band gap energy (E_g). When photons are absorbed, electrons are elevated from the valence

band states to the conduction band forming an electron/hole pair. Both the electrons in the conduction band and the holes in the valence band are mobile charge carriers. The lifetimes of these ionized states are more or less limited. Holes and electrons will recombine with some probability when they encounter each other in a radiationless process, the energy being dissipated as heat. To make use of the energy stored in the electron/hole pair, it is necessary to prevent or reduce the occurrence of recombination. This can be achieved if an electric field is present in the area where electron/hole pairs are generated. The effect of the electric field is to drive the charge carriers in opposite directions, decreasing the rate of recombination.

When a semiconductor is immersed in a liquid electrolyte solution containing a redox couple, charge transfer occurs across the interface to equilibrate the potentials of the two phases. The net result is the formation of an electric field at the surface of the semiconductor. The direction of this electric field depends on the relative electron affinities of the semiconductor and solution. The direction of the field is usually such that holes move to the surface at n-type semiconductors and lead to oxidations while in p-type semiconductors, electrons move to the surface causing reductions. Close approximations for the potentials of oxidation and reduction for the system can be calculated if the flat band potential (which for highly doped semiconductors is nearly equal to the conduction band energy, E_c, in n-type semiconductors, and the valence band energy, E_v, in

p-type) and E_g are known. However, the values of these potentials are dependent on the semiconductor, the nature of solvent used, the presence of ions which adsorb on or react with the electrode surface and the presence of surface states (34). It is useful however, to consider that under irradiation, holes and electrons have potentials corresponding to E_v and E_c respectively (35).

Table II

Band positions[a] for some common semiconductor electrodes (Ref. 36)

Semiconductor	Valence Band (volts vs SCE)	Conduction Band (volts vs SCE)
TiO_2	+3.1	-0.1
SnO_2	+4.1	+0.3
Zn_2	+3.0	-0.2
WO_3	+3.0	+0.2
CdS	+2.1	-0.4
CdSe	+1.6	-0.1
GaAs	+1.0	-0.4
GaP	+2.2	-1.0
SiC	+1.6	-1.4

a) band positions in water at pH1.

I.5.3. Principles of Operation

Theoretical treatment of semiconductor/electrolyte interfaces have been extensively covered and are available elsewhere (37-41); only a summary is given here.

When a semiconductor is immersed in a solution containing a redox couple, charge transfer occurs at the interface until equilibrium is established by equality in the Fermi levels of the semiconductor and redox couple. The amount that the Fermi level of the semiconductor shifts dictates the degree to which the bands are bent. The energy output of the photoelectrochemical cell is related to the amount of band bending to form the space charge region. The extent to which the Fermi level shifts (and band bends) determines the net voltage drop that is experienced by an electron as it passed through an external circuit to the counter electrode. This can be altered by adding an external bias to the circuit. When a semiconductor is irradiated with photons of energy $h\nu > E_g$, electron/hole pairs are produced. These pairs are separated by the electric field across the depletion layer. If the solution contains a species, D, whose solution redox potential is above that of the photo-generated holes, oxidation of the species can occur

$$D + h^+ \longrightarrow D^+ \qquad [11]$$

Figure 1. n-TYPE SEMICONDUCTOR/ELECTROLYTE JUNCTION

(Ev, valence band, edge; Ec, conduction band edge; Eg, band gap; E_f, E_{redox} and E_{fm}, Fermi levels of the semiconductor, the redox couple and metal electrode respectively; E_{fb}, flat band; E_f^*, Fermi level of illuminated semicondutor at open-circuit conditions; eV_p, photovoltage at open circuit conditions; e^-, electron; h^+, holes):

(a) before contact with electrolyte;

(b) at equilibrium in contact with electrolyte;

(c) under illumination.

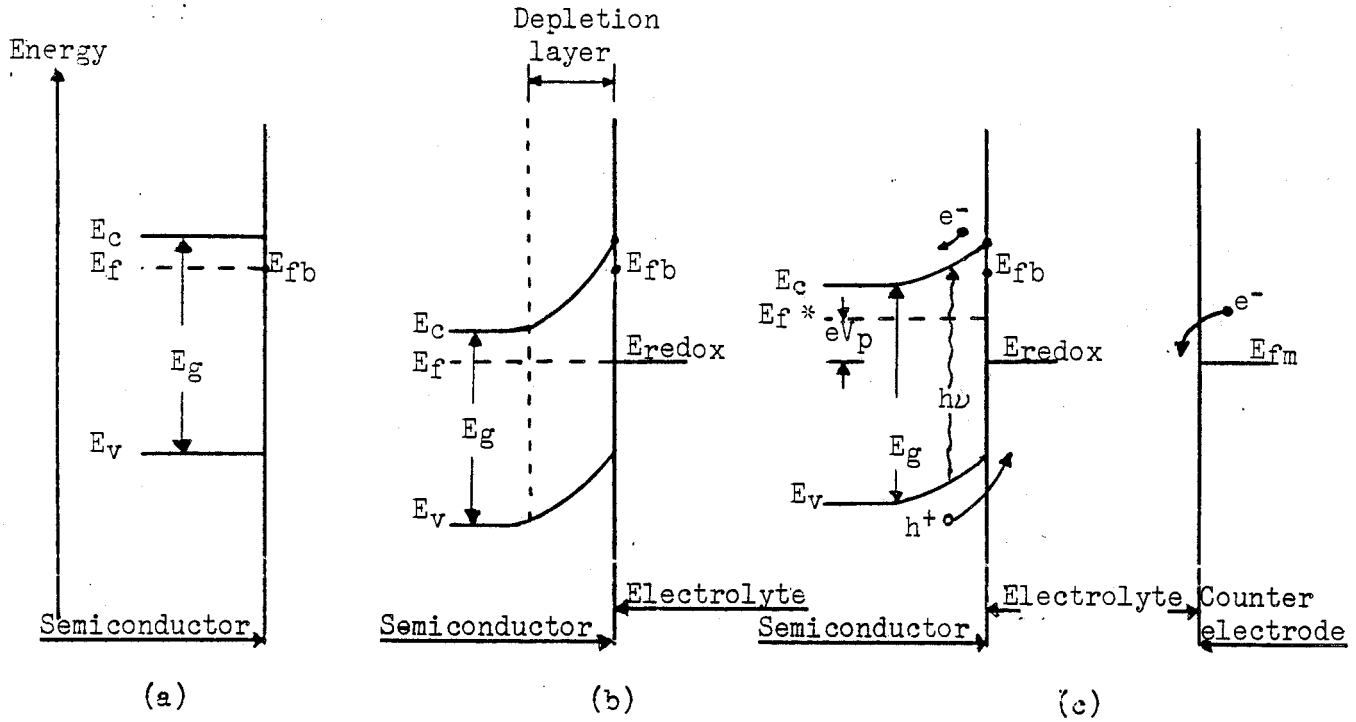
Energy
Ec
Ef
Efb
Eg
Ev
Semiconductor
(a)
Depletion layer
Efb
Ec
Eredox
Ef
Eg
Ev
Semiconductor
Electrolyte
(b)
e⁻
Efb
Ec
Ef *
eVp
Eredox
hν
Eg
Ev
h⁺
Semiconductor
Electrolyte
e⁻
Efm
Counter electrode
(c)

The electron, transferred via an external circuit to the counter electrode, reduces a species, O, to complete the reaction.

$$O + e^- \text{ ---> } O^- \qquad [12]$$

The overall reaction taking place being

$$D + O \text{ ---> } D^+ + O^- \qquad [13]$$

If the oxidized species, D^+, undergoes no further reaction at the semiconductor surface, desorption occurs and the species experiences no further influence from the photoelectrode.

Due to the presence of a band gap in a semiconductor, there is a distinction between electron transfer reactions that occur depending on whether the valence band or conduction band is involved. The relative positions of the redox levels of species in solution, with respect to the conduction and valence bands, are important as it has been shown that fast charge transfer across the semiconductor/electrolyte interface occurs when the appropriate band overlaps the redox level of the electrolyte (39). Positions of redox levels with respect to band edges have been proposed and studied in light of the selective nature of semiconductors (39,42-45).

Gerischer (46,47) has shown that in contrast to metals, the average free energy of electrons and holes in semiconductors can be changed to a large extent by illumination, especially the

Figure 2. MODEL CURRENT/POTENTIAL CURVE FOR n-TYPE SEMICONDUCTORS

Model current/potential curve for n-type semicondutors (E_{fb}, flatband potential; I_p', photocurrent):
(a) in the dark; (b) under illumination;
(c) under 50% illumination.
Region 1, cathodic current flow; Region 2, onset of photocurrent; Region 3, saturated photoanodic current.

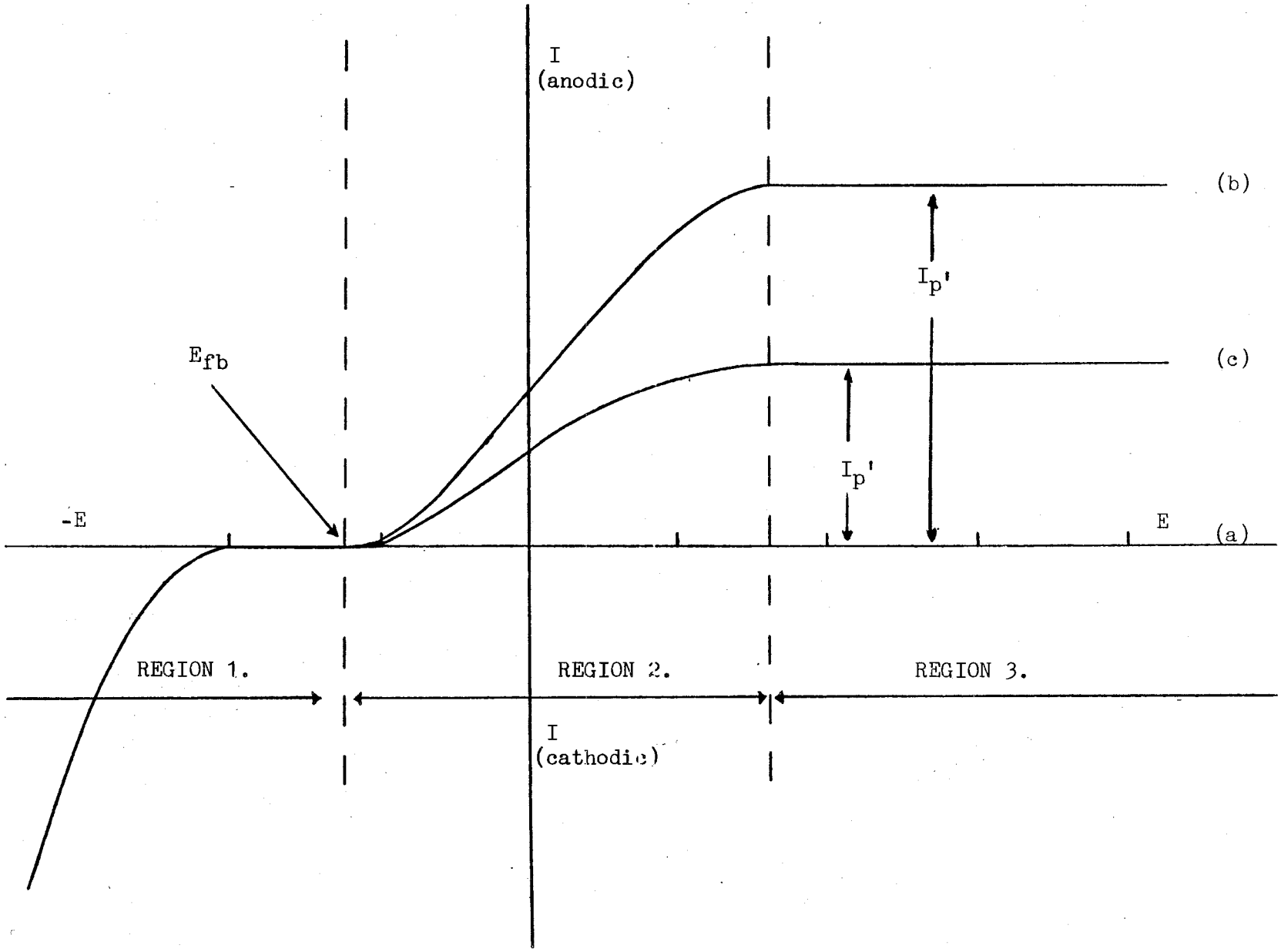
I
(anodic)
(b)
$I_{p'}$
E_{fb}
(c)
$I_{p'}$
-E
E
(a)
REGION 1.
REGION 2.
REGION 3.
I
(cathodic)

concentration of minority electronic carriers, which may differ by orders of magnitude from equilibrium values. Therefore, it is expected that most important photoelectrochemical effects in semiconductors will be due to the large change from equilibrium of the minority carriers, while the respective changes in concentrations of majority carriers will have negligible effects. Thus, the rate of oxidation at n-type and reduction at p-type semiconductors may be directly controlled with light intensity. Fig. 2 shows the model behaviour of current in a n-type photoelectrochemical cell and how it is affected by light intensity and bias voltage. Additionally, in contrast to metals, anodic biasing of n-type and cathodic biasing of p-type semiconductors does not change the working potential of the electrode. Externally applied bias to a semiconductor shifts the Fermi level in the bulk of the semiconductor, increasing or decreasing the extent of band bending. For many reactions, additional bias is applied to the system to accomplish one of the following effects

a) To increase efficiency of electron/hole pair separation by increasing the potential drop across the space charge layer.

b) To provide the counter electrode with sufficient energy to drive a reaction.

c) To provide a sufficient barrier against majority carriers reaching the electrode/solution interface.

I.5.4. Classification of Photoelectrochemical Cells

A photoelectrochemical cell is defined as a cell in which the irradiation of an electrode in contact with an appropriate electrolyte produces a change in the electrode potential with respect to a reference electrode, (under open circuit conditions) or produces a change in the current flowing in the external circuit (under short-circuit conditions) (48). A method of classifying photoelectrochemical systems has been established, based on the value and sign of the free-energy change of the total reaction which takes place in the cell (41).

I.5.4.1. Photovoltaic Electrochemical Cells

Photovoltaic cells, also known as regenerative cells (49), contain an electrolyte consisting of a single dissolved redox couple. After illumination of the semiconductor electrode, oxidation of the reduced species of the couple takes place at the photoanode (n-type) and reduction of the oxidized species of the couple occurs at the cathode. The reverse occurs in a photoelectrochemical cell when a p-type semiconductor electrode is used. The net change in solution (in theory) is zero; the composition of the electrolyte remains the same. Consequently, there is no change in free-energy of the system as the energy of the light incident on the photoelectrode is transformed into electrical energy.

I.5.4.2. Photoelectrosynthetic Cells

In these cells, light is used to drive the overall cell reaction in a non-spontaneous direction ($\Delta G>0$) so that the energy of the light is converted into storable chemical energy (eg. in fuels). In most cases, the application of an external bias to the cell is required for the process to occur or to improve the efficiency by increasing the extent of band bending thus improving the electron/hole pair separation.
Photoelectrosynthetic cells have been reported for production of hydrogen and oxygen through the decomposition of water (15,50-52)

$$H_2O \text{ ---> } H_2 + 1/2O_2 \qquad [14]$$

reduction of carbon dioxide to formic acid, formaldehyde, methanol and methane (45,53-55),

$$CO_2 + H_2O \text{ ---> } HCOOH + 1/2O_2 \qquad [15]$$

$$CO_2 + H_2O \text{ ---> } HCOH + O_2 \qquad [16]$$

$$CO_2 + 2H_2O \text{ ---> } CH_3OH + O_2 \qquad [17]$$

$$CO_2 + 2H_2O \text{ ---> } CH_4 + 2O_2 \qquad [18]$$

and the photoelectrochemical oxidation of chloride to produce chlorine (14,16,56-58).

$$2H^+ + 1/2O_2 + 2Cl^- \text{ ---> } H_2O + Cl_2 \qquad [19]$$

I.5.4.3. Photocatalytic Cells

In these cells, a reaction is driven in a spontaneous direction ($\Delta G<0$) by the energy provided by the light. Radiant energy is not converted to chemical energy as in a photoelectrosynthetic cell, but rather used to overcome the energy of activation required for a reaction. Cells employing n-TiO_2 electrodes have been used to carry out the oxidation of CN^-

$$CN^- + 1/2O_2 \text{ ---> } OCN^- \qquad [20]$$

(59), carboxylic acids (to alkanes by way of the Photo-Kolbe reaction) (19-22)

$$RCOOH \text{ ---> } 1/2R\text{-}R + CO_2 + 1/2H_2 \qquad [21]$$

alcohols, and a number of organic species (59-61).
Most photoelectrochemically initiated polymerizations would be considered photocatalytic as $\Delta G<0$ for most polymerizations, the energy put into the reaction being used to overcome the activation energy barrier.

I.5.5. Photoelectrochemical Polymerizations

The possibility of employing photoelectrochemical systems for initiating polymerizations was demonstrated by Bard and his co-workers (62) in 1979 using n-TiO_2 slurries for the polymerization of methyl methacrylate. While detailed studies on the mechanism of polymerization were not conducted, previous work suggested that the initiating species were methyl radical produced at the n-TiO_2 surface by reaction of holes with acetate

Figure 3. SCHEMATIC REPRESENTATION OF DIFFERENT TYPES OF PHOTOELECTROCHEMICAL CELLS

(a) Photovoltaic cell: Light energy is used to produce electrical energy.

(b) Photoelectrosynthetic cell: Light energy is used to drive an uphill reaction ($\Delta G>0$) and is stored in the form of chemical energy.

(c) Photocatalytic cell: Light energy is used to overcome activation barriers for reactions in which ($\Delta G<0$).

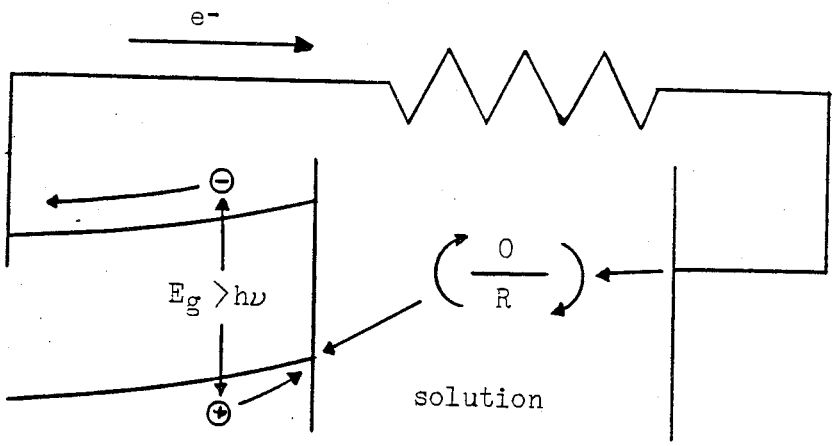

(a)

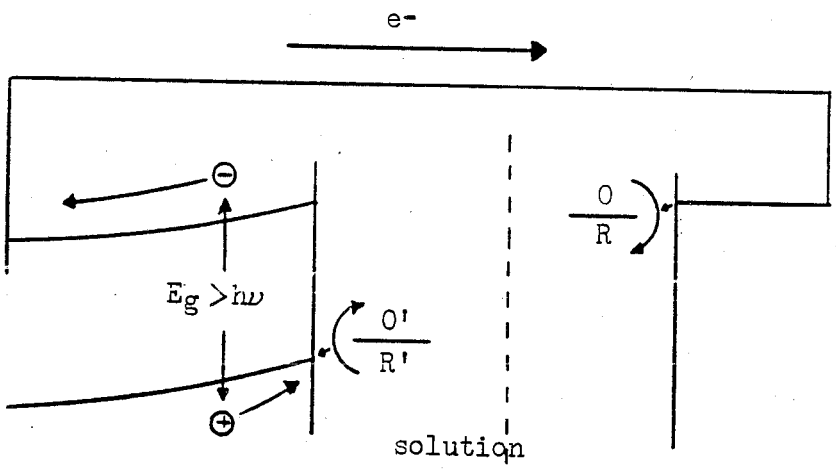

(b)

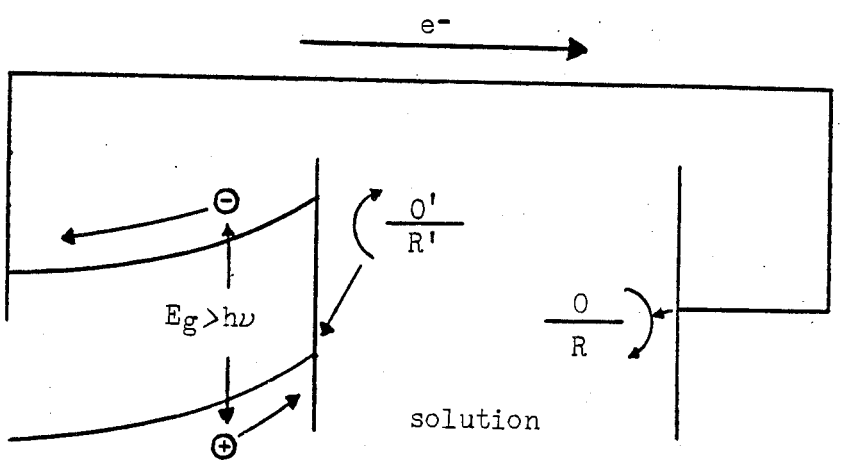

(c)

ions. Funt and Tan (63) polymerized methyl methacrylate and styrene using a polycrystalline n-TiO_2 electrode in a divided photoelectrochemical cell.

Polymer-modified electrodes have gained wide attention in recent years because of their importance in photoelectrochemical application, particularly for the purpose of corrosion suppression. The potential application of using photoelectrochemical cells to produce 3-dimensional images and coating of the semiconductor electrode with polymeric resists was suggested by both Bard (62) and Funt (63). The modification of a semiconductor by polymerizing a film directly onto a electrode surface was demonstrated by Fox et al (64); poly(vinylpyrene) was polymerized on the surface of n-GaAs using visible light irradiation. More recently, Okano, Itoh, Fujishima and Honda (65) have produced conducting patterns on semiconductor electrodes. Pyrrole was polymerized at irradiated areas of n-TiO_2 films which had been deposited on SnO_2 coated glass.

I.5.6. Photoelectrochemical Cell Designs for Polymerization

The design of a photoelectrochemical cell for polymerization must be based, in addition to semiconductor properties, on solution and polymerization properties. By considering the requirements of these three areas, potential applications and limitations come to light.

I.5.6.1. Semiconductor Properties

The main limiting factors to a semiconductor's use within a photoelectrochemical polymerization cell are the positions of the bands, the band gap energy of the semiconductor and its stability.

a) Band positions and Band-gap energy:

The values of E_c and E_v in conjunction with E_g must be such that the photo-produced minority carriers have sufficient energy to initiate the desired reaction. For ideal matching, redox energy levels should overlap the appropriate band energy level.

Large band gap materials, such as TiO_2, require UV radiation. Such semiconductors may not be suitable for the synthesis of polymers which readily photopolymerize or undergo photodegradation under UV irradiation. Semiconductors which produce minority carriers with high potentials may generate side reactions which are detrimental to polymerization.

b) Stability:

Both thermodynamic and kinetic factors influence the stability of semiconductors (30,33,66-68). Photo-produced minority carriers moving towards the semiconductor/electrolyte interface may break the bonds between the surface atoms and the electrode substrate. A number of approaches are possible to stabilize semiconductors prone to photocorrode. Electrodes that are unstable in a given electrolyte may be stabilized by adding a redox couple to the electrolyte which has a redox potential more thermodynamically favored or is kinetically favored compared to

the decomposition of the material (66,67). Modification of the surface with various films which conduct the charge from the semiconductor to species in solution has also received much attention (69,70) as a method to prevent photocorrosion. Successful applications of the same would increase the possible combinations of semiconductors and solutions that could be used.

I.5.6.2. Solution and Polymerization Properties

There are a large number of possible reactions that can occur at an electrode. A seemingly simple overall reaction may require a complex series of individual steps at the electrode. Such factors as overpotentials, adsorption onto and diffusion away from the electrode, can all play an important role in the determination of products of a electrolytic reaction. These parameters are largely dependent upon the nature of the solvent and species in solution.

The choice of experimental conditions for photoelectrochemical polymerizations would be essentially identical from a solution and polymer standpoint as those required for electrochemical polymerizations. These conditions are frequently difficult to satisfy owing to conflicting requirements of the electrolytic process on one hand and the polymerization reaction on the other. Conductivity must be sufficiently high to permit electrolysis with reasonable voltage drops across the cell; hence aqueous or at least highly polar environments are required in which a suitable supporting

electrolyte can be dissolved. The photoelectrochemical requirements of energy matching and stability also add to the difficulty in selection. Monomers and polymers, however, are mostly non-polar substances. They too must be soluble in the same solvent if the reaction is to be carried out homogeneously and with some control. In addition, solvent requirements must be considered as to the type of mechanism by which the polymerization is to be attempted. Species added to the solution to stabilize a semiconductor may be suitable for cationic polymerization but would hardly be suitable for a free radical polymerization if they acted as free radical inhibitors. Consequently, many ideal systems cannot be employed in practice due to restrictions imposed by some aspect of the photoelectrochemical or polymerization system.

It is important to note that in most electrolytic polymerizations, it is only the initiating step that can be affected by the variation of electrolytic parameters (71). Under a given set of conditions, radical polymerization of styrene should proceed by the same propagation mechanism regardless of whether it was initiated by electrolysis, photoelectrolysis, or by a chemical initiator, provided that diffusion of the initiating species from the electrode surface is fast enough and adsorption effects are negligible.

Separation of the working and counter electrodes is often required to prevent solution from moving freely between the two electrodes. Products formed at the counter electrode may react

with the initiating species or with growing chains, resulting in termination or chain transfer. Ionic polymerizations are particularly prone to such interference and separation of anode and cathode compartments for such is essential.

I.5.7. Electrolytic Control

Electroytic control, in terms of controlling the rate of initiation, may be achieved in photoelectrochemical cells through selection of light intensities. Reactions occurring at the electrode will be governed by the energy levels of the bands as well as selectivity of the semiconductor. Therefore, for a first approximation, redox potentials of species to be added to solution should be matched to the potentials of the bands. Due to the large diversity of possible electrode reactions, it is useful to use a classification scheme such as Yamazaki's (71) to categorize the reactions. Electrode reactions are divided into two major categories, cathodic and anodic. The cathodic reactions, leading to reduction products, could occur at p-type materials where the photo-produced minority carriers are electrons.

a) Generation of free radicals.

i) $H^+ + e^- \text{ ---> } H^\cdot$ [22]

ii) $CH_3\text{-}\overset{\overset{O}{\|}}{C}\text{-}C_6H_5 + e^- + H^+ \text{ ---> } CH_3\text{-}\overset{\overset{OH}{|}}{\dot{C}}\text{-}C_6H_5$ [23]

iii) reduction of oxidizing agents (peroxides)

$H_2O_2 + e^- \text{ ---> } OH^- + OH^\cdot$ [24]

$ROOR + e^- \text{ ---> } OR^- + OR^\cdot$ [25]

b) Generation of radical anions.

i) indirect electron transfer to monomer

$$Na^{+} + e^{-} \longrightarrow Na \qquad [26]$$

$$Na + M \longrightarrow Na^{+} + M^{\cdot -} \qquad [27]$$

ii) direct electron transfer to monomer

$$M + e^{-} \longrightarrow M^{\cdot -} \qquad [28]$$

c) Formation of unstable monomer.

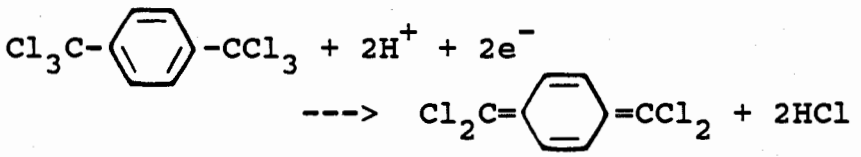

[29]

d) Formation of an active catalyst.

i) $Fe^{+3} + e^{-} \longrightarrow Fe^{+2}$ [30]

$Fe^{+2} + H_2O_2 \longrightarrow OH^{-} + OH^{\cdot} + Fe^{+3}$ [31]

ii) $Ni^{+2} + 2e^{-} \longrightarrow Ni^{0}$ [32]

The anodic reactions, leading to oxidation products, could occur at n-type electrodes where the photo-produced minority carriers are holes.

e) Formation of free radicals by the Kolbe reaction.

$$R\text{-}COO^{-} \longrightarrow R\text{-}COO^{\cdot} + e^{-} \longrightarrow R^{\cdot} + CO_2 + e^{-} \qquad [33]$$

f) Formation of cation radicals.

i) indirect electron transfer from monomer

$$ClO_4^{-} \longrightarrow ClO_4^{\cdot} + e^{-} \qquad [34]$$

$$ClO_4^{\cdot} + M \longrightarrow ClO_4^{-} + M^{\cdot +} \qquad [35]$$

ii) direct electron transfer from monomer

$$M \longrightarrow M^{\cdot +} + e^{-} \qquad [36]$$

g) Ring opening polymerization initiated by direct or indirect electron transfer from monomer.

h) Oxidative condensation polymerization.

$$F^- \text{ ---> } F^{\cdot} + e^- \quad [37]$$

$$F^{\cdot} + C_6H_6 \text{ ---> } FH + C_6H_5^{\cdot} \quad [38]$$

$$2C_6H_5^{\cdot} \text{ ---> } C_6H_5\text{-}C_6H_5 \quad [39]$$

Electrolytic initiation often implies a significant degree of control over the rate of the initiation reaction. This can be demonstrated using the example of a reduction/oxidation initiator system, such as described by equations [30-32]. The hydroxyl radicals produced by the reaction of hydrogen peroxide with ferrous ion initiate the polymerization of a vinyl monomer. Taking advantage of electrolysis, one may start with an inactive system comprised of Fe^{+3} ions and H_2O_2 and produce the required amount of active Fe^{+2} ions by electrolytic reduction. Variations in the current would be reflected in variations in the concentration of Fe^{+2} and thereby in the rate of initiation. From this point of view, the electrolytic method possesses a great degree of flexibility as to the instantaneous control of initiator concentration.

Following is a summary of beneficial characteristics and potentials of electrolytic polymerizations initiated photoelectrochemically.

a) In addition polymerizations, the electrolytic reaction generally participates in the initiation process and not in the propagation reaction.

b) By externally controlling the photocurrent, it is possible to program the course of a reaction where the concentration of initiator and rate of polymerization determine the molecular weight and molecular weight distribution of the polymer, thus tailoring the properties of the final polymer.

c) Termination of growing ends in living polymer systems can be controlled by current switching.

d) Photoelectrochemical oxidation and reduction of appropriate functional groups leading to condensation polymerization.

e) Active catalytic complexes can be prepared in situ by the electrolytic oxidation of inactive components resident in the polymerization system.

f) Control of initiation rates with light intensity without affecting the potential of the minority carriers.

g) Preparation of polymer-modified electrodes.

h) Image formation of both polymeric conductors and resists on semiconductor surfaces.

II. EXPERIMENTAL METHODS

II.1. Chemicals and Their Purification

Reagent grade acrylamide (Polysciences) was recrystallized in a Soxhlet extractor using a mixed solvent of 2:1 n-heptane to acetone. The acrylamide was dried under vacuum and stored in the dark over calcium chloride ($CaCl_2$) until used. Monomer purified in this manner showed no traces of residual polymer.

Ethyl vinyl ether (EVE) (Polysciences) was filtered through a column of activated alumina and subsequently stirred over fresh CaH_2 for 24 hours before being refluxed and distilled on a spinning band distillation column. The middle fraction was collected and stored below 0 °C in the dark under a blanket of N_2.

Isobutyl vinyl ether (IBVE) (Kodak) was treated and purified in the same manner as ethyl vinyl ether. Sulfuric acid (BDH), sodium sulfate (BDH), acetic acid (Fisher), and sodium acetate (BDH) were all of reagent grade and were used without any further purification. Tetraethylammonium perchlorate (Kodak) was recrystallized twice from water. The tetraethylammonium perchlorate (TEAP) was then dried under vacuum for several hours and stored in a tightly sealed container. Tetrabutylammonium perchlorate (MCB), reagent grade, was dried under vacuum and stored over $CaCl_2$ in dark until used.

Water used for solvent was singly distilled and deionized by passing it through a Barnstead Ultrapure (mixed) deionizing column. The water was then clarified, to remove suspended

particles, by filtering it through a Waters filter assembly using a 0.45 μm pore size type HA filter.

Acetonitrile (Caledon HPLC grade) was stirred and refluxed for several hours over fresh CaH_2. The acetonitrile was then fractionally distilled under a N_2 atmosphere. It was collected and stored over activated molecular sieves.

Dichloromethane (Fisher spectrometric grade) was filtered through a column of activated alumina and subsequently refluxed over CaH_2 for several hours before fractional distillation on a spinning band column. The middle fraction was collected and stored under a blanket of N_2 until used.

II.2. Photoelectrochemical Cells

The cell used for the initial polymerization experiments is shown in Fig. 4. The cell was equipped with a side arm from which samples of solution could be withdrawn. A rubber septum, fitted to the end of the sidearm, made it possible to remove solution samples with a syringe during the course of an experiment. The design of the cell was such that N_2 could be bubbled through or passed over the solution. A flat quartz window was built into the cell to allow the photoanode to be illuminated. To separate the anode and cathode compartments, a sleeve was used to house the counter electrode. A porous glass disk was used to separate the solutions of the working and counter electrode compartments.

Figure 4. THE PHOTOELECTROCHEMICAL CELL

1 - quartz window; 2 - semiconductor electrode;
3 - reference electrode; 4 - counter electrode;
5 - sampling port; 6 - nitrogen inlet.

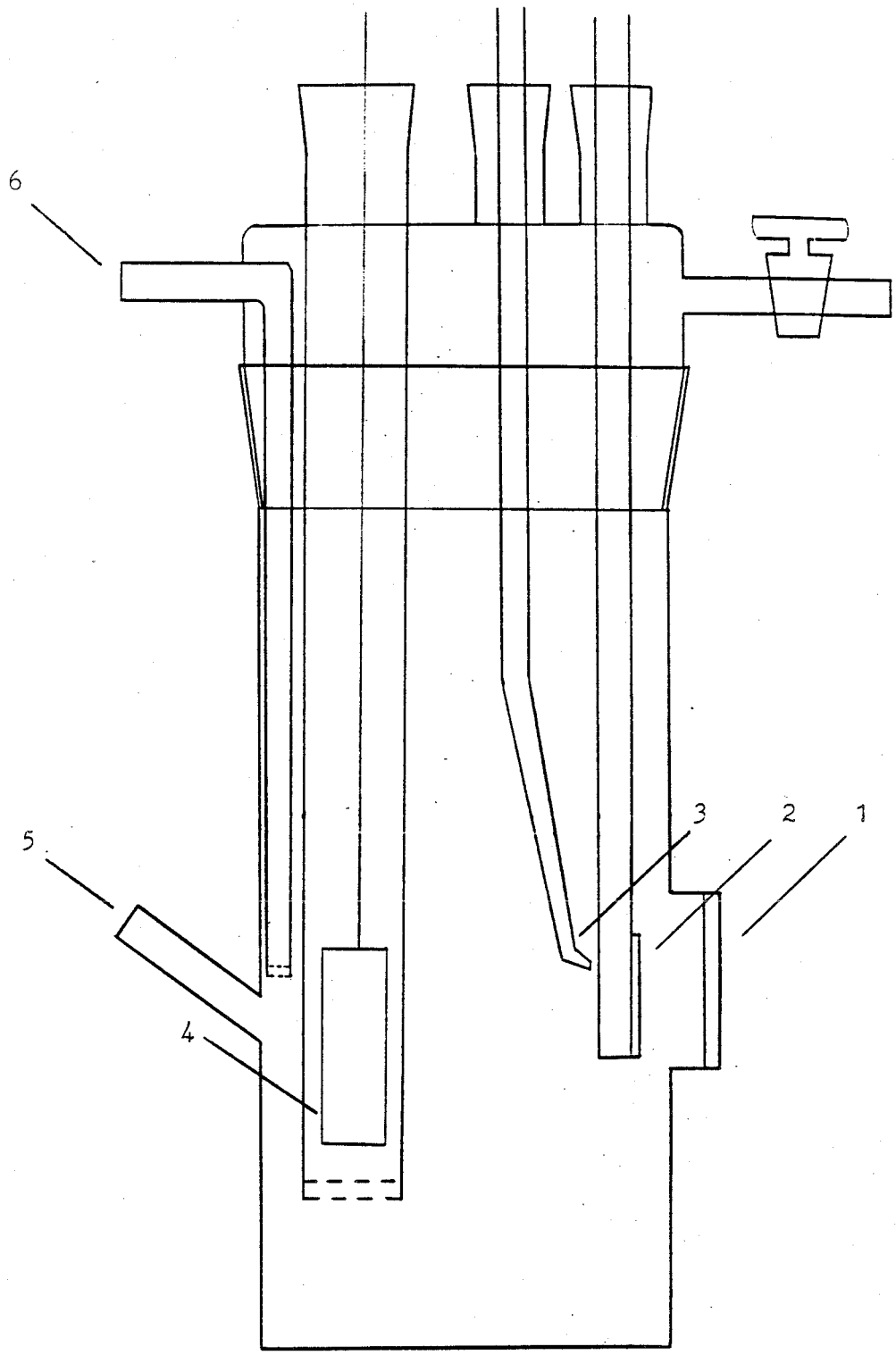
6
5
4
3
2
1

Electrodes employed in the photoelectrochemical experiments were constructed of n-type TiO_2 single crystals. Crystals were etched in molten sodium hydroxide before the electrode was assembled. Electrical contacts were made by rubbing the back of the crystals with an indium/gallium alloy. Ohmic contacts were confirmed by measuring the resistance between two contacts on the back of the crystal. A shielded wire was connected to the contacts using Electrodag. The crystal was finally mounted on a glass tube support with "five minute" epoxy leaving the (100) face exposed. The tubing was fitted to the cell using a standard tapered glass tubing adapter. Electrodes for use in non-aqueous solvents were constructed using Contac 24 hour epoxy and cured for 24 hours at 60 °C.

A saturated calomel electrode (SCE) was used regularly as a reference electrode. The SCE was separated from solutions in the working electrode compartment by means of an agar gel salt bridge. A one inch square of platinum foil was used as the counter electrode.

II.3. Illumination Techniques

An optical bench was used to ensure that alignment of the lamp and cell was the same for all experiments. Illumination for the photoanode was delivered by an Illumination Industries 200 watt high pressure mercury lamp. The lamp was equipped with a quartz collimating lens. In all experiments, the light beam was passed through a quartz filter, containing water, to remove heat due to infrared radiation. A 3 inch by 3 inch square filter

holder was used to hold cutoff filters as required. A Corning #3966 filter which cuts off at 300 nm was used for all acrylamide experiments unless otherwise specified. A 2 inch by 2 inch square filter holder was used to house neutral density filters as required. The photoelectrochemical cell, which had been coated with black paint on the exterior to exclude unfiltered light, was immersed in a thermostatically controlled constant temperature bath. The total assembly, including the optical bench, was housed in a box which could shield the system from other light sources.

II.4. Characterization of Photoanodes

n-TiO_2 single crystals were used for the electrode material of the photoanodes for the entirety of this work. Electrode pieces were cut from a large single crystal bullion so as to expose the (100) face to solution. The cut pieces were doped with niobium to produce the n-type material. The doped samples were dark blue in color, almost black. This coloration denoted a heavy concentration of donor impurities. The dopant level, N-$10^{19}/cm^3$, and flat band potentials, E_{fb}=0.0 volts vs SCE, were determined in aqueous solutions of saturated KCl. Cutting of the crystal, doping as well as determination of dopant level and flatband potentials were done in the SFU physics department.

Electrodes were washed with distilled water and acetone after each use. After being washed, the electrodes were stored in an oven at 60 °C until used. When it became apparent, either through visual inspection or a decrease in performance, that the

Figure 5. EXPERIMENTAL ALIGNMENT

1 - Hg lamp; 2 - heat filter; 3 - filter holder; 4 - constant temperature bath; 5 - photoelectrochemical; cell; 6 - working electrode; 7 - reference electrode; 8 - counter electrode; 9 - to constant temperature circulator; 10 - from constant temperature circulator; 11 - quartz window; 12 - optical bench.

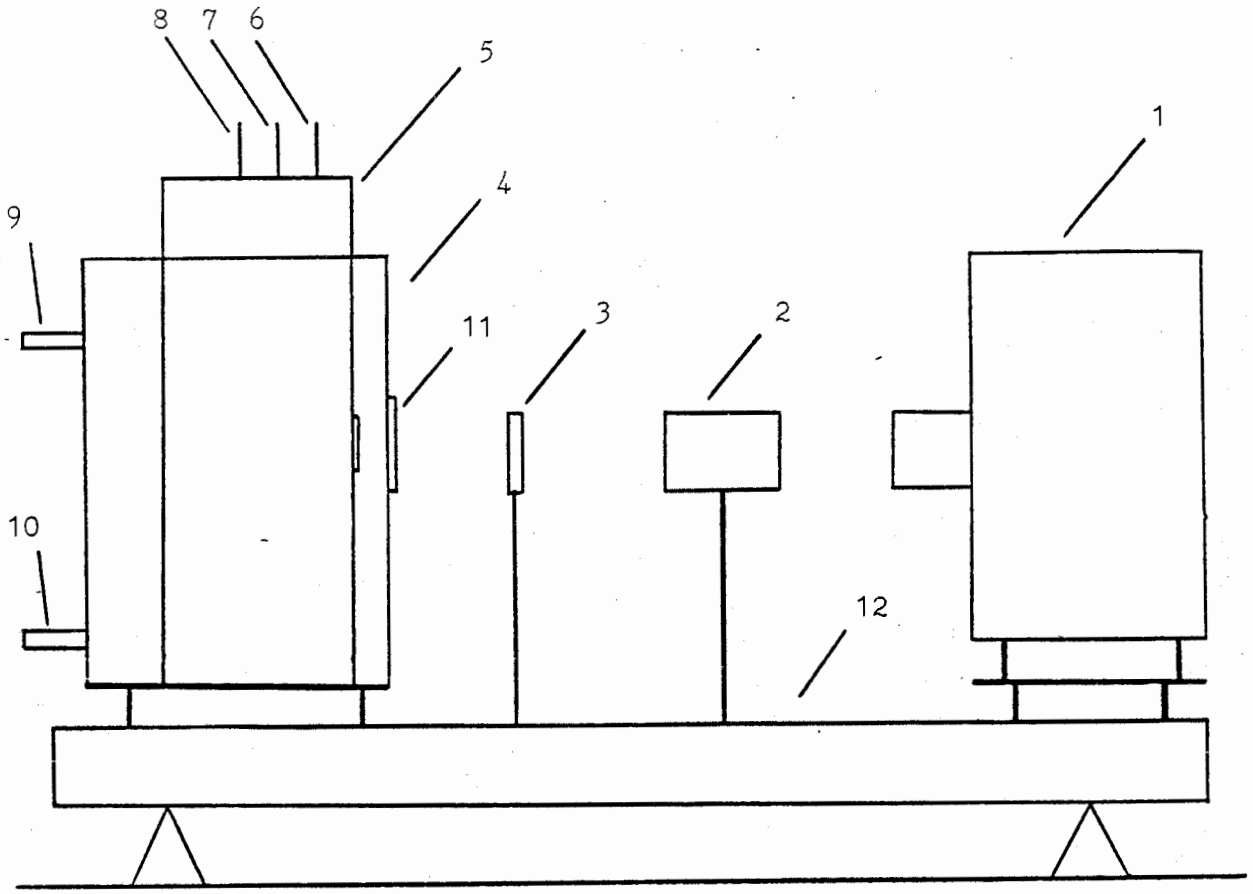
8
7
6
5
4
9
11
3
2
1
10
12

electrodes had deteriorated, the bonding material of the electrode was stripped away and the crystal cleaned in hot chromic acid for one hour before reassembly.

The photocurrent response of the n-TiO_2 electrodes to wavelength was determined at room temperature. Photo-response was measured in an aqueous solution of 2.0 M acetic acid containing 1.0 M sodium acetate. A constant bias of 2.000 volts vs SCE was applied to the semiconductor by a PAR model 363 potentiostat. The counter electrode was a platinum sheet. Response was measured in a two compartment cell of the type shown in Fig. 4. The solution was deareated with N_2 before photo-response was measured. Current was monitored with a Fluke model 8840 multimeter. A Kratos monochromator was used in conjunction with a Kratos 200 watt high pressure mercury lamp. Intensity of the various wavelengths of light was monitored with a YSI Kettering model 65A Radiometer using a thermopile detector.

Photocurrent as a function of light intensity was measured in an aqueous, 2.0 M acetic acid - 1.0 M sodium acetate, solution. The experiment was conducted at room temperature in a two compartment cell using a platinum counter electrode. A bias of 2.000 volts vs SCE was kept on the photoelectrode by a PAR 363 potentiostat. Intensity of a Illumination Industries 200 watt Hg lamp was changed using Oriel neutral density filters. Currents at several light intensities were measured with a Fluke 8840A multimeter.

Current-Voltage (I/V) curves, for the following solutions were recorded:

a) 0.10 M H_2SO_4 in water

b) 2.0 M acetic acid - 1.0 M sodium acetate in water

c) 0.10 M tetraethylammonium perchlorate in acetonitrile

d) 0.10 M tetrabutylammonium perchlorate in dichloromethane

The potential of the photoanode was controlled with a PAR model 179 potentiostat. Cycling of applied bias was regulated with a PAR 175 programmer or a BAS Cyclic Voltammetry unit. Cycling rates of 50 and 100 millivolts per second were employed. Plots were recorded on a Allen XY recorder.

II.5. Polymerization Procedures

Prior to addition of monomer to solvent and electrolyte, I/V curves were normally recorded to establish the condition of the photoanode. If the electrode was in good working order, monomer was added to the cell and N_2 bubbled through the solution for a minimum of 15 minutes prior to passage of current. During experiments involving acrylamide in aqueous solutions, N_2 was bubbled continuously throughout the experiment to remove oxygen produced at the n-TiO_2 photoelectrode. Experiments involving non-aqueous solvents had bubbling terminated prior to the start of the polymerization and the solution blanketted by a flow of N_2 across the top of the cell.

Initial experiments used a bias of 0.100 volts vs SCE on the semiconductor electrode and were conducted in a one compartment cell. All subsequent polymerizations were done in a two compartment cell, so as to separate the anode and cathode. A bias voltage of 2.000 volts vs SCE was applied to the photoanode with the exception of the polymerizations in dichloromethane in which the potential used was 3.000 volts vs SCE. A PAR 363 potentiostat was used to apply bias for experiments conducted in aqueous solutions and a PAR 173 potentiostat for non-aqueous solutions. Coulometric data was recorded with a PAR 179 coulometer. Currents were monitored with a Fluke 8840A multimeter.

Solution samples were withdrawn with a syringe via the sidearm at regular intervals during an experiment. The concentration of acrylamide was determined by gas chromatography (GC) analysis. Ethyl vinyl ether and isobutyl vinyl ether concentrations were monitored by infrared absorbance. Polymers were isolated from solution at the termination of an experiment by precipitation of the polymer. Polyacrylamide was precipitated from solution by pouring an aliquot into 800 ml of methanol. Poly(ethyl vinyl ether) (PEVE) and poly(isobutyl vinyl ether) (PIBVE) were precipitated out of solution with distilled water.

II.6. Gas Chromatography Analysis

The concentration of acrylamide was determined using a Hewlett Packard 5710A GC. Concentrations were determined using an internal standard of n-butanol in methanol, the methanol being

used as a solvent and a precipitant for polymer in the samples to exclude polyacrylamide from being injected into the GC. Volumes of 1 to 3 microlitres of sample were injected into the GC. Analysis was done using a 18 inch long, 1/8 inch stainless steel column packed with Poropak Q. The injector temperature was 300 °C. Oven temperature was programmed to start at 150 °C, increase at a rate of 8 °C per minute to 200 °C and hold for 8 minutes. Helium carrier gas flow was set at 30 millilitres per minute. A Flame Ionization Detector using a hydrogen-air flame was heated to 350 °C. The analog signal from the GC was sent to an Apple IIe computer equipped with an Interactive Microware Inc. (IMI) Adalab card which received and converted the analog signal to digital. IMI's Chromatochart software was used to calculate retention times and peak areas from which monomer concentrations were determined.

II.7. Infrared Spectroscopy

Infrared spectroscopy was used for two purposes; a) to calculate the concentration of ethyl vinyl ether and isobutyl vinyl ether and b) for identification of polymers. Both ethyl vinyl ether and isobutyl vinyl ether have absorption peaks around 1210 cm^{-1} which are characteristic of the monomers and not of the polymers. Standard calibration curves of absorbance were made at 1210 cm^{-1} for both monomers. It was determined from the standard calibration curves that this technique was useful for determining the monomer concentration of ethyl vinyl ether to 0.02 M and isobutyl vinyl ether to 0.05 M. Solutions of tetraethylammonium

perchlorate in acetonitrile and tetrabutylammonium perchlorate (TBAP) in dichloromethane were checked for absorbance in the 1210 cm^{-1} range. No absorbance of either of the two solutions in the 1210 cm^{-1} region was found.

A Wicks analytical cell with NaCl windows was used for the monomer concentration analysis. Samples removed from the polymerization cell were injected directly into the infrared cell and spectrum run immediately to determine absorbance due to monomer.

Films of polyacrylamide for IR were prepared by evaporation of polymer from a solution of water onto Mylar sheets. Films made in this manner were dried under vacuum to remove residual water. Poly(ethyl vinyl ether) and poly(isobutyl vinyl ether) films were prepared from solutions of chloroform deposited on sodium chloride windows. Spectra were recorded on a Perkin Elmer 599B Infrared Spectrometer.

II.8. Molecular Weight Analysis.

Molecular weights of polyacrylamide samples were determined by dilution viscosity techniques. Molecular weights and molecular weight distributions of poly(ethyl vinyl ether) and poly(isobutyl vinyl ether) were measured by GPC. A Waters Associates' model 301A gel permeation chromatograph, employing a differential refractometer detector was used to measure the molecular weights and distribution of poly(ethyl vinyl ether) and poly(isobutyl vinyl ether) samples.

Intrinsic viscosities of polyacrylamide samples were determined with a Ubbelohde type viscometer using 1.0 N sodium nitrate solution. The viscometer and polymer solutions were thermostatically held at 30.0 °C. Intrinsic viscosities were obtained by extrapolation to infinite dilution of reduced viscosity values. The relation $[n] = KM^a$ was used to determine the weight average molecular weights of the polymers. Values of $K=6.80 \times 10^{-4}$ and $a=0.66$ were used (72). Values of molecular weights calculated using the dilution technique were compared to those using a one point viscosity technique (73). Good agreement was found when low concentrations of polymer were used. Reported molecular weights were calculated using the one point technique.

For molecular weight determinations of polyethers, the GPC was equipped with three Styragel columns of the following pore dimensions: 100,000 Å; 10,000 Å; and 1,000 Å. All measurements were carried out in toluene at 30 °C. Constant flow rate of 2 ml/minute was used throughout.

Samples containing approximately 0.5 grams of polymer per 100 ml of solution were used for analysis. Solutions were filtered under pressure through Millipore Teflon filters to remove impurities and undissolved polymer particles. Two hundred microlitres of sample solution were injected into the GPC via the sample loop.

The columns were calibrated with a series of narrow molecular weight distribution polystyrene (PS) samples from Waters Associates and Polyscience Inc. The calibration graph

is a plot of the log of the peak molecular weight of the sample against its GPC elution volume.

Calibration curves for poly(ethyl vinyl ether) and poly(isobutyl vinyl ether) were constructed based on the polystyrene curve. It is generally accepted that log([n])(MW) is a constant for all polymers in a given solvent at the same temperature and elution volume (1). It is possible to write the equation

$$\log [n]_x MW_x = \log [n]_s MW_s \qquad [40]$$

in which x and s indicate the unknown polymer and the standard polymer respectively. By replacement of each intrinsic viscosity term by its Mark-Houwink expression

$$[n]_j = K_j MW^{a}_j \qquad [41]$$

and solving the resulting equation for log MW_x, the expression which describes the elution volume calibration curve for MW_x is obtained

$$\log MW_x = \frac{1}{1 + a_x} \log \frac{K_s}{K_x} + \frac{1 + a_s}{1 + a_x} \log MW_s \qquad [42]$$

Literature values for the K and a values for polystyrene,

poly(ethyl vinyl ether) and poly(isobutyl vinyl ether) at 30 °C are known (74).

	K	a
Polystyrene	1.05×10^{-2}	0.72
Poly(ethyl vinyl ether)	1.82×10^{-2}	0.85
Poly(isobutyl vinyl ether)	2.50×10^{-2}	0.80

Substituting K and a values into equation [42], the expressions needed to construct the calibration curves for poly(ethyl vinyl ether) and poly(isobutyl vinyl ether) can be obtained.

$$\log MW_{PEVE} = -0.1291 + 0.9297 \log MW_{PS} \qquad [43]$$

and

$$\log MW_{PIBVE} = -0.2093 + 0.9730 \log MW_{PS} \qquad [44]$$

The analog signal from the GPC detector was sent to an Apple IIe computer equipped with an IMI Adalab card which performed the analog to digital conversion. IMI's Chromatochart and GPC Enhancement software were used in conjunction with the Apple IIe to calculate the molecular weights and molecular weight distributions.

Peak elution times were determined for some polyacrylamide samples using the GPC. Three Micropak TSK exclusion columns, with exclusion limits of 300,000 800,000 and 8,000,000, were installed in the GPC for retention time measurements of polyacrylamide samples. Polymer samples of approximately 0.10 grams were dissolved in 25 ml of an aqueous solution of 0.36 M acetic acid

0.04 M sodium sulfate and approximately 0.1 ml/litre of the wetting agent Rexal-25J. Samples were filtered and injected into the GPC in the same manner as the polyethers. Pump rate for polyacrylamide samples was 1.0 ml/minute. The signal from the detector was recorded on a Fisher Recordall stripchart recorder running at a chart speed of 2.0 cm/minute. No suitable standards were available in order to establish a calibration curve for the polyacrylamide samples.

III. RESULTS AND DISCUSSION

III.1. Characterization of Photoanodes

III.1.1. Introduction

Since Fujishima and Honda reported the photoelectrolysis of water using TiO_2, many researchers have extensively studied TiO_2 and other semiconductors in liquid junction configurations (75-81). Among the factors that determine the efficiency and usefulness of photoelectrochemical systems for given applications are the thickness of the space charge layer at a specified potential, the flatband potential and optical properties of the semiconductor, the recombination mechanism of photogenerated carriers, the electron transfer mechanism to a substrate in solution and the concentration and identity of the dopant species. As these parameters strongly influence the shape of the light induced I/V curve, the following characteristics of the n-TiO_2 electrodes were examined

a) The photocurrent response of the electrode with respect to wavelength.

b) The photocurrent response to light intensity.

c) The effect of solvent and supporting electrolyte on the shape of the photo-induced I/V curve.

TiO_2 was chosen as the n-type semiconductor for this work for two particular reasons. First, it was desired that the photo produced minority carriers would have sufficient energy so as not to limit the operating range of potential of the

photoelectrochemical cell. The 3.0 eV band gap of TiO_2 with a flatband potential of approximately 0 volts vs SCE provides holes with high oxidation potentials. Second, TiO_2 has proven to be extremely stable as a photoelectrode material. Many semiconductors are limited in use due to poor stability and susceptibility to poisoning. TiO_2 appeared to be relatively free of these detrimental effects (30,48,66-68). Platinized powders and polycrystalline electrodes both contain a high degree of grain boundaries, edges and damaged sites which act as recombination centers for the photo-produced electron/hole pairs. Wilson, Harris and Gerstner (82) have investigated the photoelectrochemical behaviour of TiO_2 (rutile) as a function of damage on the electrode surface. Their findings indicated that increased damage to the surface of TiO_2 electrodes resulted in a decrease in current and quantum efficiency, $\emptyset_q$

$$\emptyset_q = \frac{N(e)}{N(h\nu)} \qquad [45]$$

where N(e) = the number of electrons flowing in the external circuit and $N(h\nu)$ = the number of incident photons of energy $h\nu$.

Reproducibility is best enhanced with the use of single crystal electrodes. Surface damage can be minimized through etching, electrode areas readily determined and coulometric data recorded. For these reasons, single crystal electrodes of n-TiO_2 were used for this work.

III.1.2. Photoresponse as a Function of Wavelength

Anodic current began to flow for wavelengths shorter than 410 nm, that is 3.03 eV, which corresponds to the band gap of TiO_2. For heavily doped samples of n-type semiconductors, the Fermi level can be considered to be approximately equal to the energy of the conduction band at flatband conditions. Using this approximation, at a pH = 4.5, the energy of holes for the TiO_2 electrode would be ca. 3.4 volts vs a normal hydrogen electrode (NHE).

Several reports have appeared in which the spectral absorbance of TiO_2 was modified through use of dyes and various dopants (15,79,82-84). Spectral shifting, if stability and energy of holes were maintained, could be advantageous for photoelectrochemical initiations where UV light would cause photopolymerization or degradation of the polymer.

Data for the photo-response curve was corrected for two effects. First, the intensity of light from the Hg lamp was normalized for each wavelength. Second, the background current measured under dark conditions (dark conditions being defined as the absence of light of with energy > 3.0 eV) was subtracted from the photocurrent. The resulting photoresponse curve for TiO_2 electrodes is shown in Fig. 6.

III.1.3. Photocurrent Response to Light Intensity

Nozik (85), and Mavroides et al. (86) reported the effects of light intensity on the performance of photoelectrochemical

cells using n-type TiO_2. Both demonstrated that the photocurrent responded linearly with light intensity to the point at which photocurrent saturation occurred. The level at which this occurs is to a large extent dependent on the dopant density and the depth of the space charge region. Higher concentrations of impurities within the electrode provide more sites for photon absorbance, increasing the intensity level at which saturation is reached. The photocurrent response, as shown in Fig. 7, was linear with respect to changes in light intensity. No saturation of the electrode was noted up to an intensity of 750 mW/cm^2.

Quantum efficiency, calculated using an average energy of 3.50 eV per photon, was 0.45. The implication of the quantum efficiency value is that 45 % of the photons reaching the surface of the electrode result in electrons that can be measured flowing through the external circuit of the photoelectrochemical cell. Several of the contributing factors that cause deviation from unity for quantum efficiency are reflectance off the surface of the electrode, recombination of holes and electrons in the bulk of the electrode, recombination at surface states and the presence of photons with energy less than that of E_g within the Hg light.

III.1.4. Current/Voltage Curves

The model for light induced I/V curves is characterized by three regions as shown in Fig. 2 for a n-type semiconductor. Region 1 is associated with cathodic current production and is relatively independent of light. The area enclosed within region 2

Figure 6. SPECTRAL DISTRIBUTION OF PHOTOCURRENT

In aqueous solution of 2.0 M acetic acid - 1.0 M sodium acetate; applied bias of 2.000 volts vs SCE.

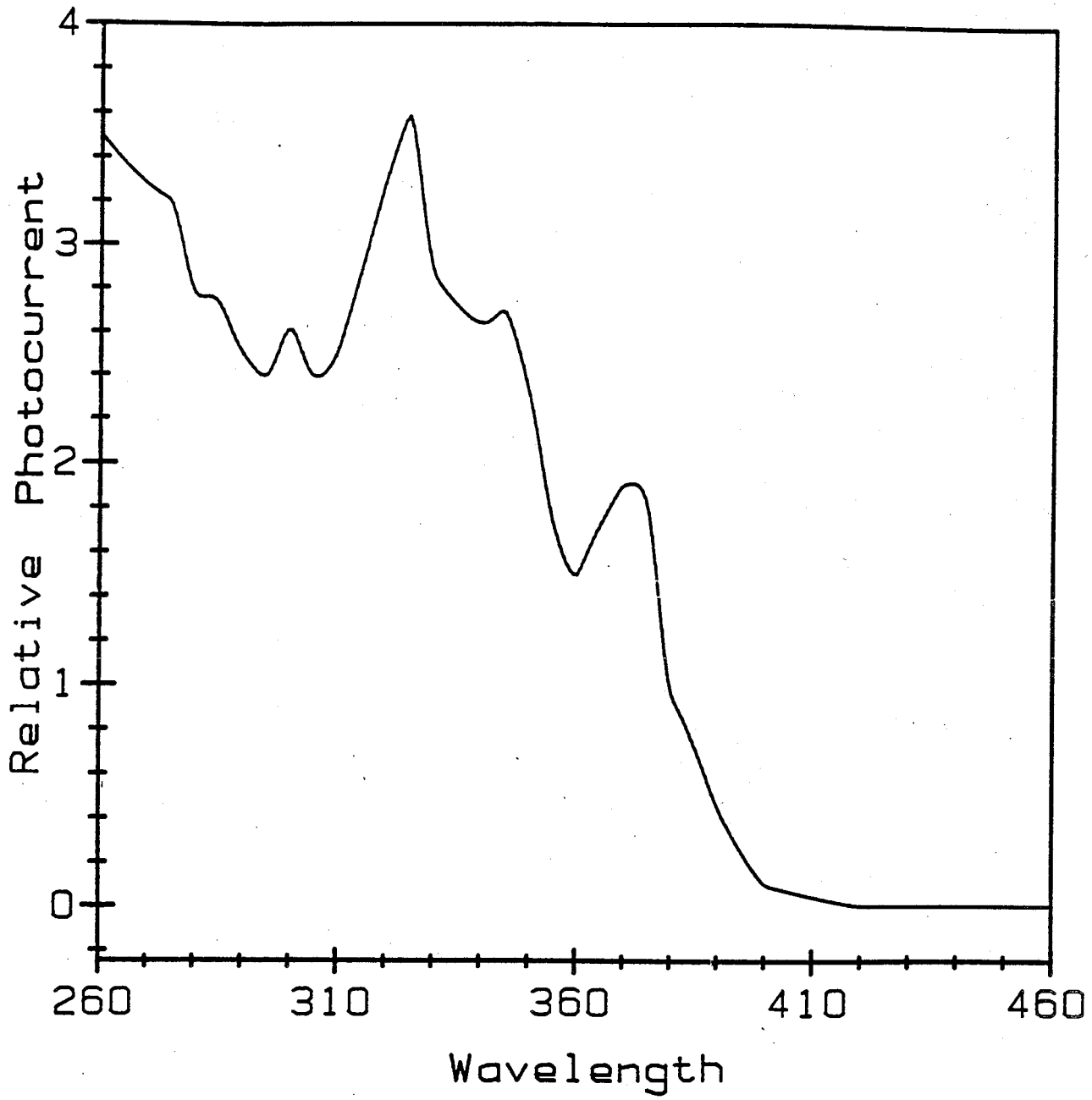
4
3
2
1
0
Relative Photocurrent
260
310
360
410
460
Wavelength

Figure 7. PHOTOCURRENT RESPONSE TO LIGHT INTENSITY

In aqueous solution of 2.0 M acetic acid - 1.0 M sodium acetate; applied bias of 2.000 volts vs SCE.

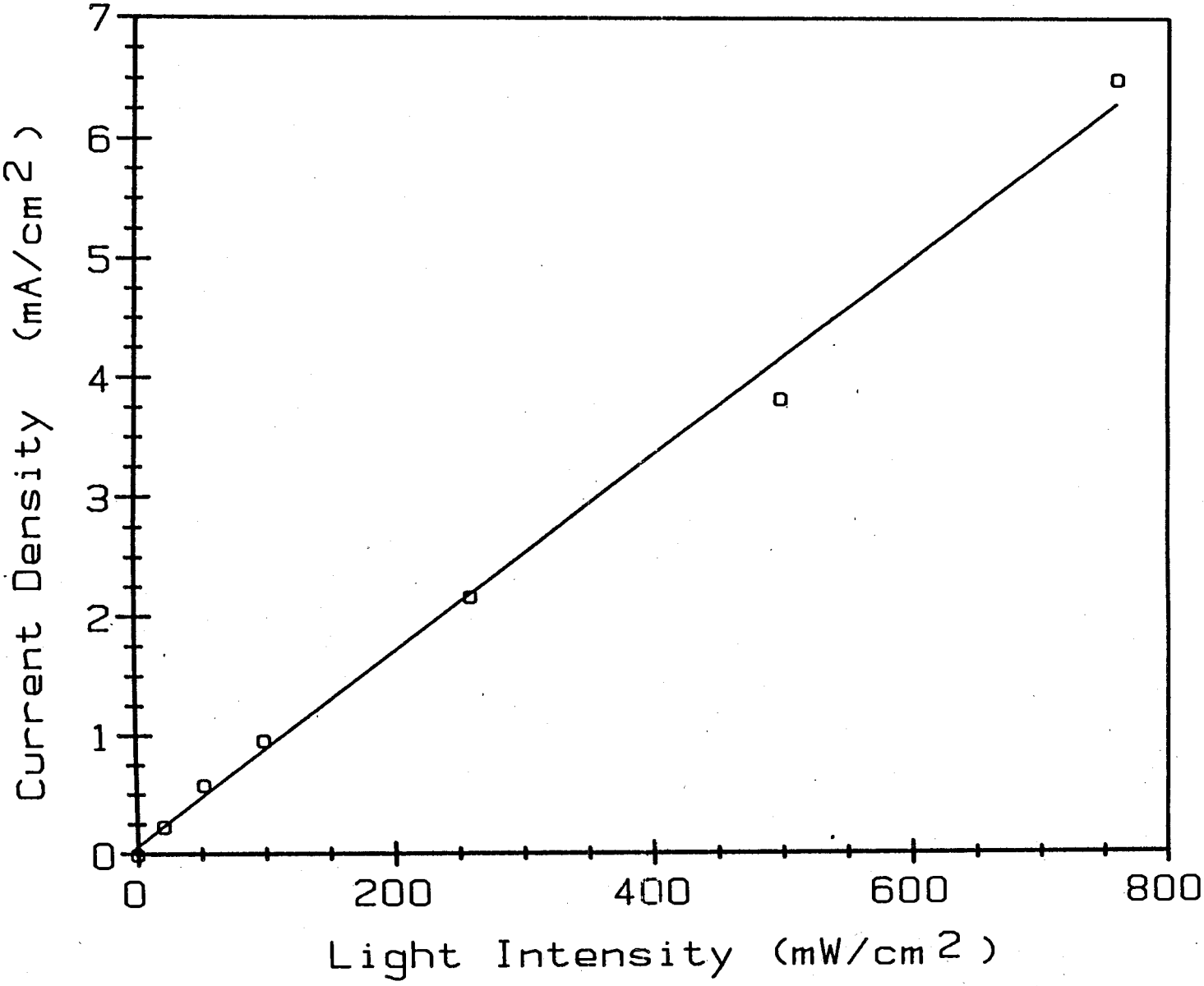
Current Density (mA/cm 2)
0
1
2
3
4
5
6
7
0
200
400
600
800
Light Intensity (mW/cm 2)

begins at the onset of anodic current and extends to the point at which current begins to level off. Region three encompasses the plateau region where anodic current changes very little with an increase in anodic bias to the potential at which electronic breakdown of the crystal begins. Within region 2, anodic current begins to flow as photo produced holes react with solution species at the electrode surface. As the bias is increased, the potential across the space charge region is increased as the bands are bent to a greater degree. The potential drop across the layer is such that electrons flow towards the bulk of the semiconductor and holes to the surface. A plateau region is reached, region 3, when the space charge region reaches the point where all electron/hole pairs, created by absorption of photons within the depletion layer and a holes diffusion length from the depletion layer are separated and the potential across the layer is sufficiently large to prevent electrons from passing through to the surface of the electrode. Once the potential reaches the point at which the plateau region is established, increases in potential have little effect until the potential becomes great enough to cause anodic breakdown of the electrode.

In the dark, Fig. 8, no current flows as the potential is made more positive than E_{fb} as few holes are created to accept the electrons from a species in solution. At very high potentials, the phenomenon of breakdown begins to occur. The potential at which breakdown occurs is a function of dopant density; the greater the concentration of impurities, the lower

the potential at which breakdown will occur. Anodic breakdown of TiO_2 as shown on the I/V curve (dark conditions), Fig. 8, begins about 3 volts vs SCE.

The light induced I/V curves for aqueous solutions, Figs. 9 and 10,show the three characteristic regions of I/V curves with a slight sloping of the curve in the plateau region. The I/V curve produced under light conditions for the acetonitrile solution, shown in Fig. 10, also possesses the three regions characteristic of I/V curves. However, the overall shape of the I/V curve is notably different, particularly the high slope of the curve through the plateau region. The light induced I/V curve for the dichloromethane solution, Fig. 11, varies considerably from that of the model curve. The transition between region 2 and 3 of the I/V curve is particularly difficult to distinguish but appears to be within the range of 1.7 to 2.0 volts vs SCE.

Low conductivity of non-aqueous solutions may be responsible for the lack of adherence to a model I/V curve. Voltage drops across the cell resulting from the higher solution resistances could account for the excessive slope of the curve through the plateau portion of the curve.

The mechanism of electron transfer from a semiconductor electrode to a species in solution is dependent upon the nature of the solvent and presence of ions which adsorb on, or react with the semiconductor surface. Electron transfer, between a n-TiO_2 electrode and a species in solution, is believed to be a

Figure 8. DARK CURRENT/POTENTIAL CURVE FOR AQUEOUS SOLUTION

Supporting electrolyte 2.0 M acetic acid - 1.0 M sodium acetate.

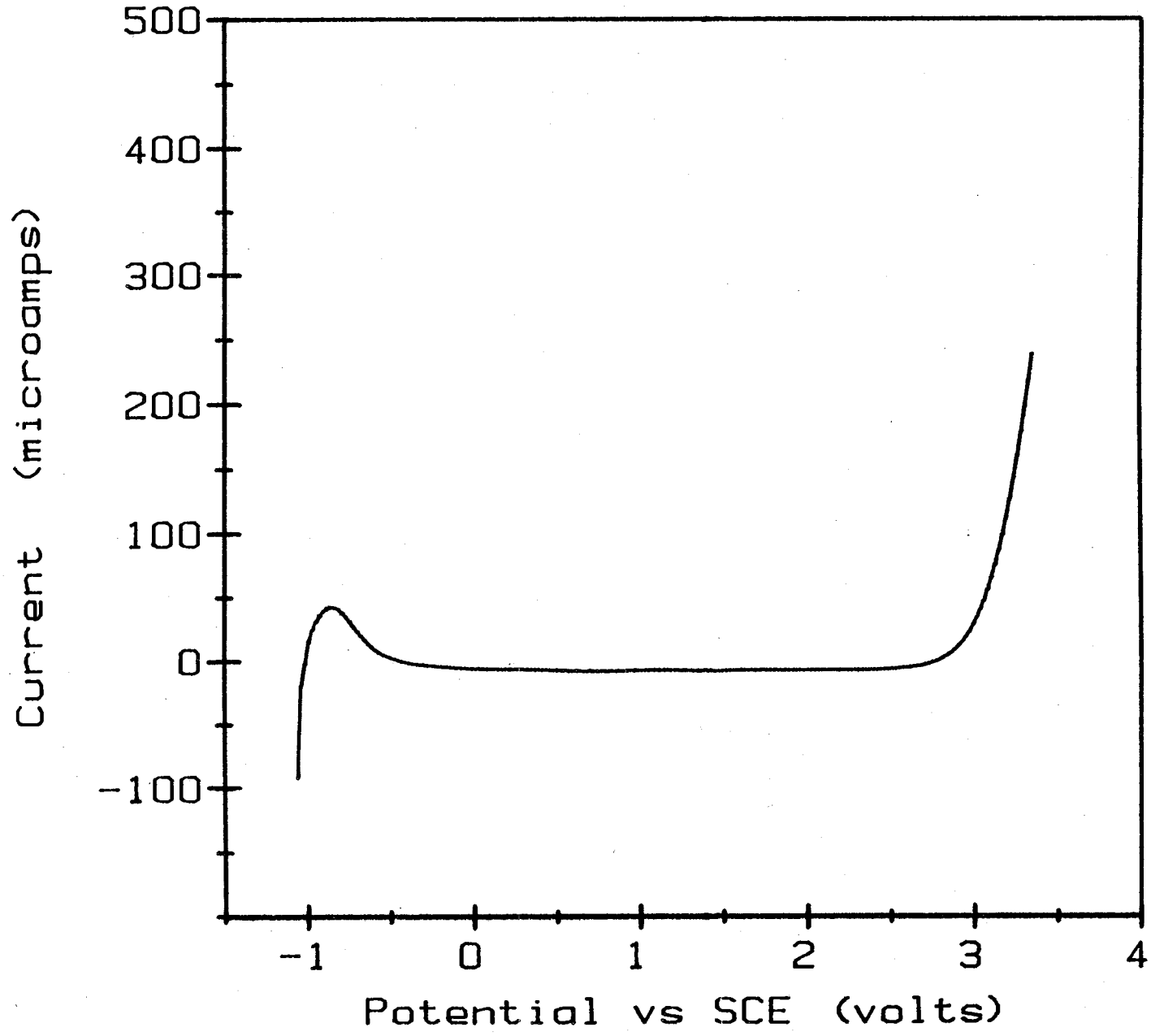
500
400
300
200
100
0
-100
Current (microamps)
-1
0
1
2
3
4
Potential vs SCE (volts)

Figure 9. CURRENT/POTENTIAL CURVE FOR AQUEOUS SOLUTIONS

(a) Supporting electrolyte 0.50 M H_2SO_4.

(b) Supporting electrolyte 2.0 M acetic acid - 1.0 M sodium acetate.

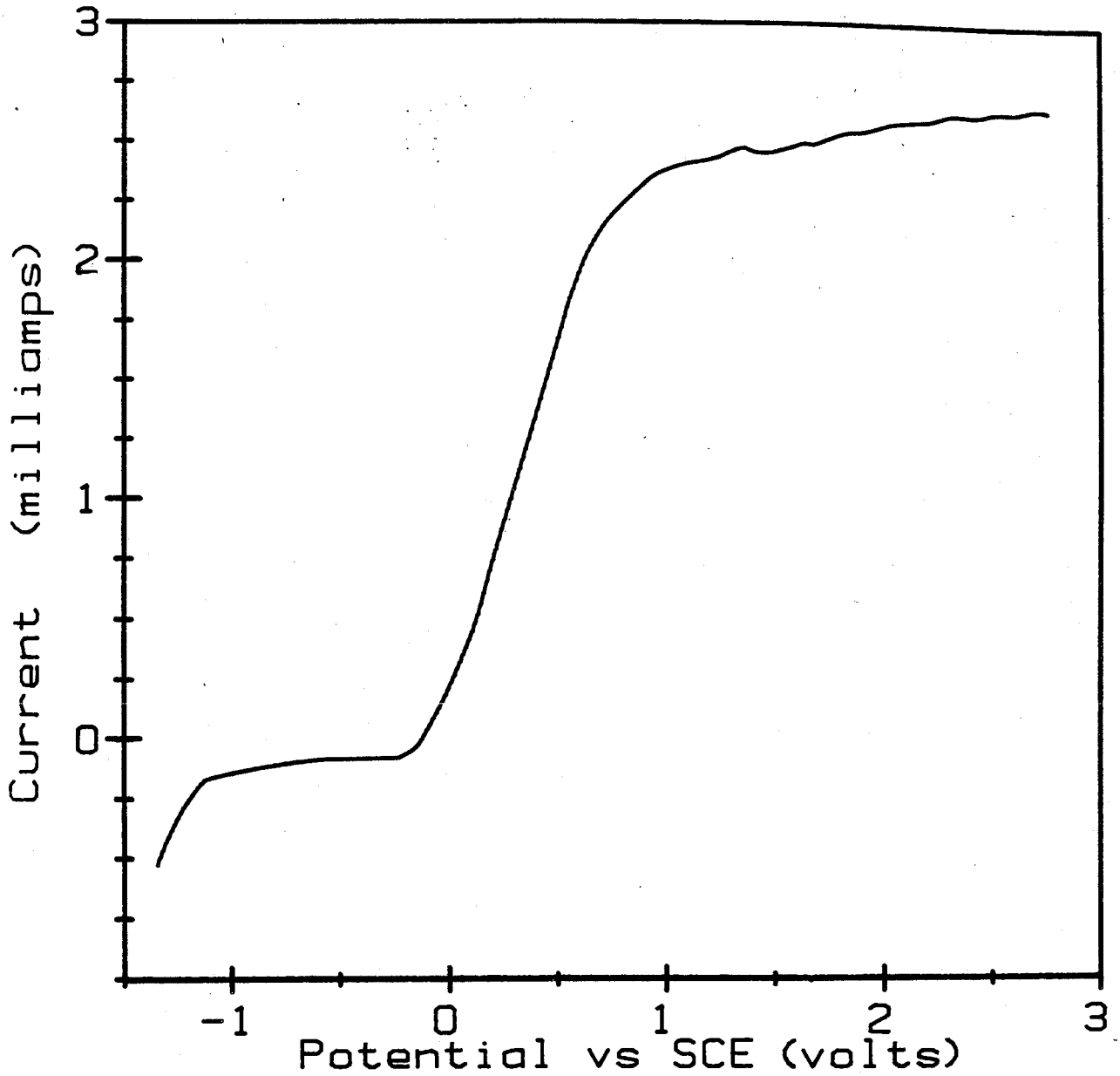

(a)

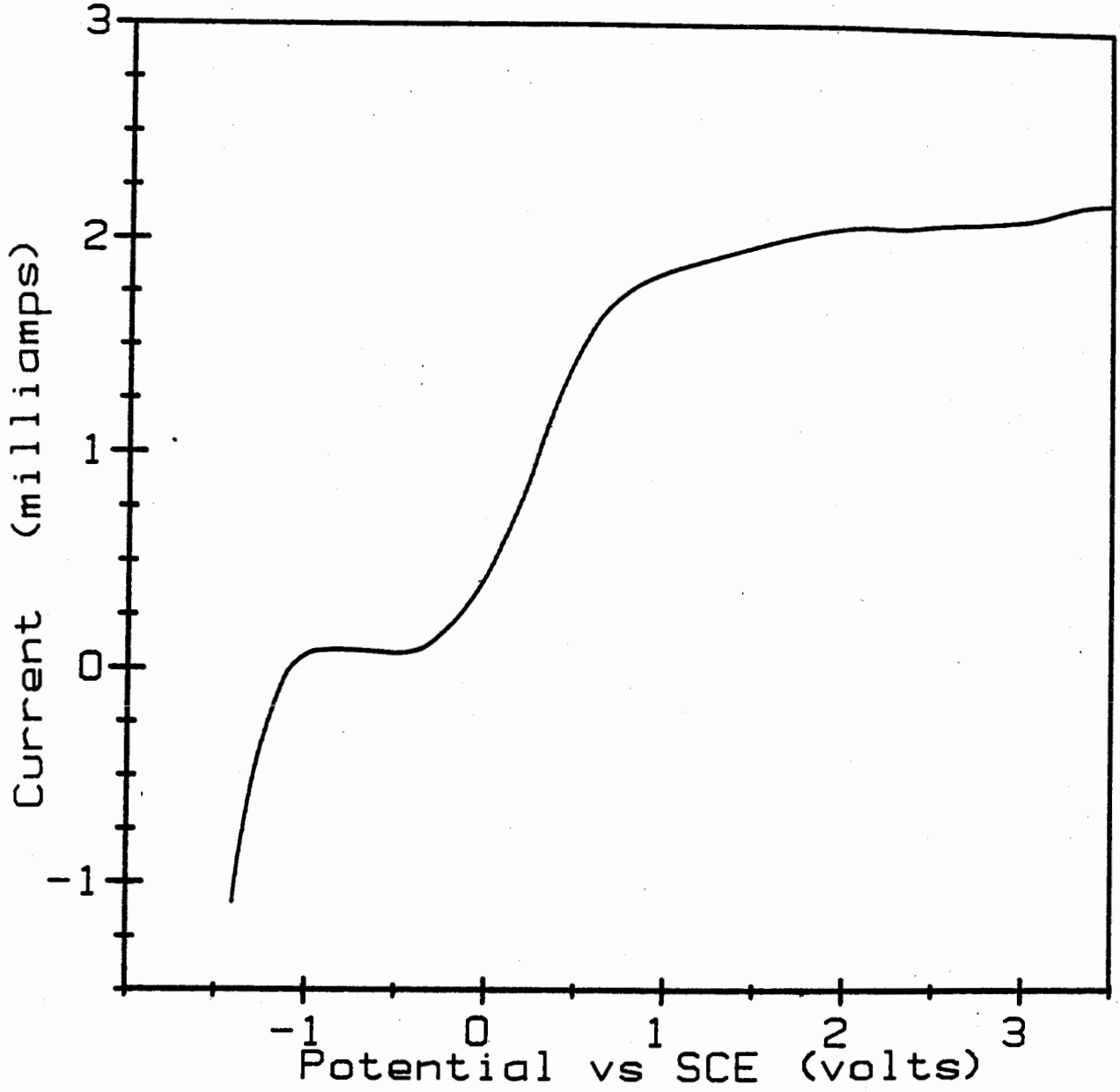

(b)

Figure 10. CURRENT/POTENTIAL CURVE FOR ACETONITRILE SOLUTION

Supporting electrolye 0.10 M tetraethylammonium perchlorate.

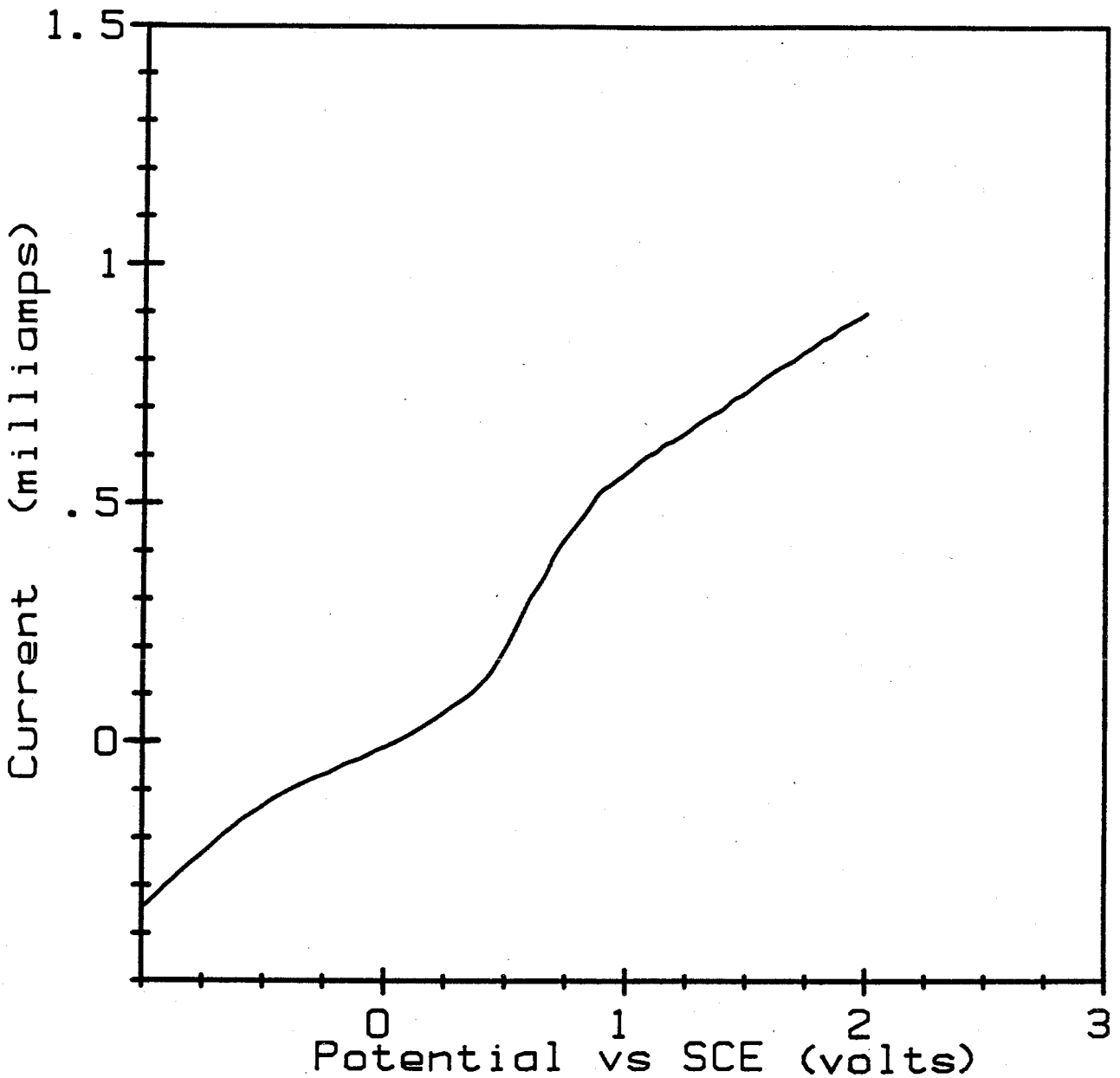
1.5
1
.5
0
Current (milliamps)
0
1
2
3
Potential vs SCE (volts)

Figure 11. CURRENT/POTENTIAL CURVE FOR DICHLOROMETHANE SOLUTION

Supporting electrolyte 0.10 M tetrabutylammonium perchlorate.

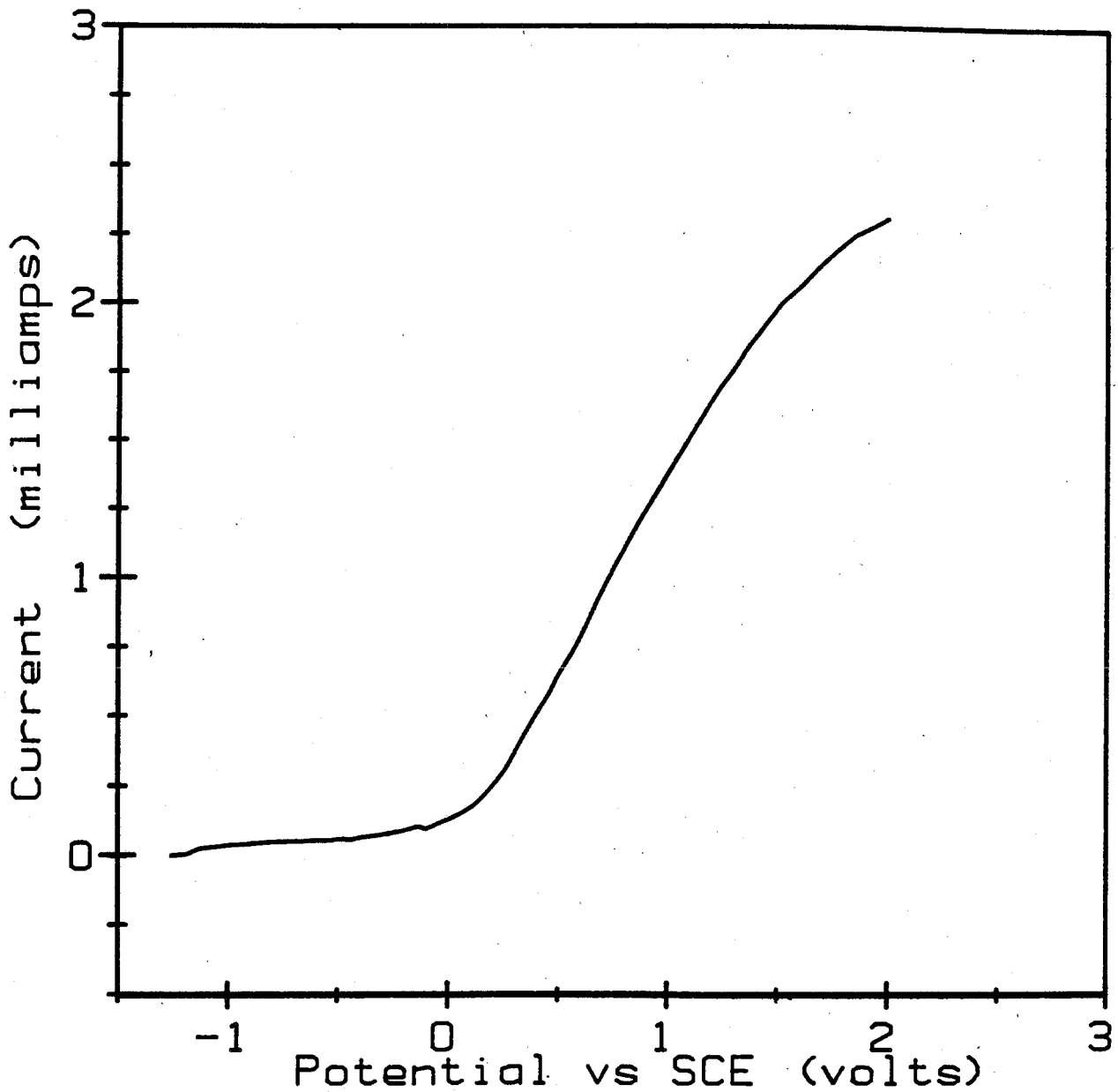
Current (milliamps)
3
2
1
0
-1
0
1
2
3
Potential vs SCE (volts)

multiple step process in which water, adsorbed to the surface of the electrode, plays an essential role in the electron transfer process (51,58,67). As the presence of water is detrimental to cati polymerizations, purification techniques are designed to minimize residual concentrations of water in all materials used. The extremely low concentration of water within the photoelectrochemical cell may play an undetermined part in influencing the shapes of the acetonitrile and dichloromethane light induced I/V curves.

III.2. Polymerization of Acrylamide

III.2.1. Initial Experiments

Initial experiments were performed to determine the feasibility of polymerizing acrylamide photoelectrochemically. As n-TiO_2 is known to readily produce O_2 through the splitting of water, N_2 was bubbled for the duration of experiments conducted in aqueous solutions. The data for initial polymerizations of acrylamide is presented in Table III. With unfiltered Hg light focused on the photoelectrode, a conversion of 54.0% of monomer was obtained. A second experiment, performed without the photoanode in solution, resulted in a conversion of 10.4% due to photoinitiation. No polymerization occurred under dark conditions in the presence of a biased n-TiO_2 electrode, nor was any charge measured to have passed through the cell. Of the 54.0% of acrylamide converted in the first experiment, it was calculated, by difference, that 43.6% of the conversion was due to a

photoelectrochemical event, 10.4% due to a photochemical event and 0.0% due to an electrochemical event. Similar competitive photo and photoelectrochemical reactions in the process of polymerization were also reported by Bard (62) and Funt (63). To eliminate the shorter ultraviolet components of the Hg light, ultraviolet cutoff filters were employed. The ultraviolet absorbance spectra of acrylamide solutions were checked to determine the appropriate cutoff filter. An increase in ultraviolet absorbance at 300 nm indicated that a filter which

Table III

Summary of initial photoelectrochemical polymerizations of acrylamide

Expt.	Irradiation conditions[a]	Average current	Photoanode	Polymer yield (%)
A1	unfiltered	4.5 mA	YES	54.0
A2	unfiltered	0.0 mA	NO	10.4
A3	none	0.0 mA	YES	0.0
A7	filtered[b]	0.0 mA	NO	0.0
A8	filtered[b]	3.3 mA	YES	28.0

a) Hg high pressure light source.
b) 300 nm cutoff filter.

blocked light of energies greater than 300 nm should eliminate monomer photopolymerization. In an experiment in which Hg light, filtered through a Corning #3966 filter, was used to illuminate

the photoanode, 28.0% of monomer was converted to polymer. In the absence of the photoanode, no monomer conversion resulted. Monomer concentrations were determined by GC analysis. An increase in the viscosity of solution during the course of polymerization was accompanied by a decrease in monomer concentration. Polymer was precipitated, as a white featherlike substance, by pouring an aliquot of polymerized solution into methanol. Comparison between the amount of precipitate collected and the decrease in monomer concentration indicated that polymerization was responsible for the decrease in monomer concentration. The infrared spectrum of photoelectrochemically produced polyacrylamide is shown in Fig. 12.

The fact that acrylamide is not susceptible to cationic polymerization and water is not a suitable solvent for cationic polymerization (1,6,) suggests that the polymerization proceeded by way of a free-radical mechanism. To further clarify the mechanism, oxygen, a free-radical inhibitor, was added to the polymerization system. The polymerization solution was first deaerated with N_2 followed by saturation with O_2. No polymerization could be detected in solutions saturated with O_2. The inhibition of polymerization establishes the free-radical nature of the acrylamide polymerization. Lack of reproducibility of polymerization, attributed to O_2 production during photoelectrolysis, occurred in systems which were not continuously purged with N_2. Gomes et al. (14), Bard and Kraeutler (19), Fujishima, Honda et al. (16,58,87), and others

Figure 12. INFRARED SPECTRUM OF POLYACRYLAMIDE

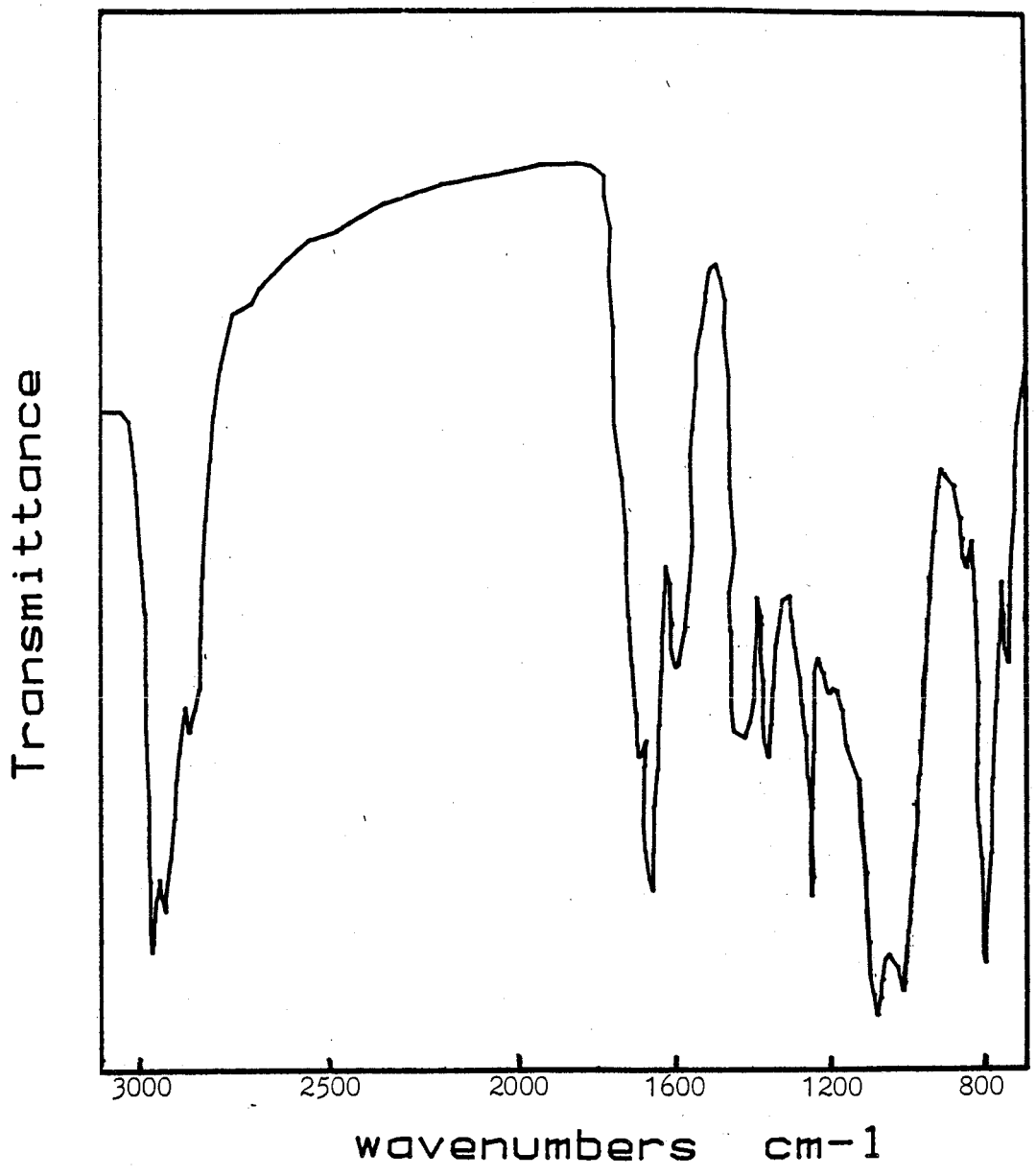
Transmittance
3000
2500
2000
1600
1200
800
wavenumbers cm-1

(88,89) have investigated the competition between several anions and water for the holes of n-TiO_2. Addition of a species to the polymerization system which would compete with the oxidation of water and initiate polymerization, would be beneficial in reducing the production of O_2. The presence of such a competitive substrate could also increase the efficiencies of the photoelectrochemical system.

The radical responsible for initiating the polymerization of acrylamide, may be a hydroxyl radical, hydrogen radical or sulfate anion radical produced by one of the following reactions

$$OH^- + h^+ \longrightarrow OH^\cdot \qquad \text{at anode} \qquad [46]$$

$$SO_4^{-2} + h^+ \longrightarrow SO_4^{\cdot -} \qquad \text{at anode} \qquad [47]$$

$$H^+ + e^- \longrightarrow H^\cdot \qquad \text{at cathode} \qquad [48]$$

All three radicals are well known to be initiators of free radical polymerizations (1,90). Of the three, $H^\cdot$ initiation could be tested by separating the anode and cathode into separate compartments. In a divided photoelectrochemical cell, $H^\cdot$ initiation would occur exclusively in the cathode compartment. Distinguishing between $SO_4^{\cdot -}$ as the initiating species would be more complex. Although spin trapping and Electron Spin Resonance experiments could possibly be used to determine the presence of each of the radical species, identification of the initiator species would not be confirmed. Determination of initiators by polymer end group analysis, may identify the initiator but this

is not always possible due to the low concentration of ends if the degree of polymerization is large. The possibility also exists that polymerization may be initiated by both the hydroxyl radicals and sulfate radical anions.

III.2.2. Variation in Supporting Electrolyte

As the mechanism of electron transfer from a semiconductor electrode to a species in solution is dependent upon the solvent and ions in solution, several supporting electrolytes were tried in conjunction with the photoelectrochemical polymerization of acrylamide. A change in supporting electrolyte could result in a notable change in efficiency as anions of the electrolytes may have different affinities for the holes of n-TiO_2. Acrylamide was polymerized using the following supporting electrolytes: sulfuric acid, sodium sulfate, tetraethylammonium perchlorate and acetic acid - sodium acetate. The polymerization using sulfuric acid has been reported in the previous section. Data for polymerization for all four electrolyte solutions are reported in Table IV. Polymerization of acrylamide occurred with each of the supporting electrolyte solutions. The results of the polymerization using tetraethylammonium perchlorate as the supporting electrolyte demonstrated that hydrogen radicals did not initiate polymerization as polymer was formed exclusively in the anode compartment of a divided cell. Hydroxyl radicals produced at the electrode surface as a step in the oxidation of water are the most probable source of initiation in the solution containing tetraethylammonium perchlorate. Although perchlorate radicals can

initiate cationic polymerization in non-aqueous solutions, the very high oxidation potential and reactivity of the perchlorate radicals with water to produce perchloric acid (11,91),leave little likelihood that $ClO_4^{\cdot}$ was the initiating species. However, this does not suggest that sulfate radicals were not involved in the polymerization of acrylamide in solutions where SO_4^{-2} was present as the anion of the supporting electrolyte. The formation of sulfate radical anions, through the oxidation of adsorbed sulfate ions on $nTiO_2$, has been supported by investigations in the corrosion of TiO_2 photoanodes (66,67). Evidence correlating the corrosion of the electrodes with the presence of sulfate ions has led to the suggestion that photocorrosion is due to the formation of sulfate radical anions. To prevent corrosion of the photoanode, the radical anions must be scavenged from the electrode surface. If the acrylamide monomer proved to be an adequate scavenger, the radical anions scavenged off the surface of the electrode could initiate polymerization.

The majority of anodically produced free-radical polymerizations reported have been confined to the generation of radical species involving the Kolbe electrosynthesis, particularly of acetate anions (11,92-94). The electrochemical polymerization of acrylamide in aqueous solutions of tartaric acid (95), acetic acid with potassium acetate (96) and trifluoroacetic acid with potassium trifluoroacetate (97,98)

Table IV

The effects of supporting electrolyte systems on the polymerization of acrylamide

Supporting electrolyte	Bias vs SCE	Charge passed (coulombs)	Current density (mA/cm^2)	Electrode area (cm^2)	Polymer yield %
H_2SO_4 [a]	0.100	11.88	6.6	0.50	28.0
Na_2SO_4 [a]	0.100	8.60	4.8	0.50	14.5
TEAP [b]	0.100	13.68	6.8	0.50	27.7
HOAc-NaOAc [b]	2.000	0.486	1.6	0.083	54.9

a) using a single compartment cell.
b) using a two compartment cell.

through Kolbe electrolysis has been reported. The report by Bard, Kraeuthler and Reiche of the polymerization of methyl-methacrylate is the first published account of polymerization initiated via Kolbe photoelectrosynthesis in which the anodic oxidation of the carboxylate anion was accomplished in a photoelectrochemical cell (62). The polymerization of acrylamide in an aqueous solution of acetic acid plus sodium acetate reported here is the first known photoelectrochemical polymerization using the Photo-Kolbe reaction in an aqueous medium. Attention should be drawn to the point that experimental conditions were not identical for each supporting electrolyte system studied. The greatest variation between systems was the

amount of applied bias and the size of the semiconductor electrode used for the acetic acid - sodium acetate system. Results listed in Table V clearly show that, aside from the buffering aspect of the acetic acid and sodium acetate electrolyte, an increase in current efficiency of over 50 fold was obtained compared to the other electrolyte systems; current efficiency being defined as the moles of monomer polymerized per faraday passed. Since the energy of holes (photo-produced minority carriers) is not affected by changes in the bias applied to the electrode, the change in applied bias would not be expected to have a significant influence on current efficiencies. The increase in efficiency may be attributed to a combination of several factors. The large affinity of acetate ions for holes at the surface of TiO_2 electrodes (88), results in an increased fraction of holes producing polymerization initiators. As the current is decreased, due to the use of a smaller electrode, the rate of oxidation is decreased, resulting in a decrease in the concentration of methyl radicals. When the concentration of initiator is lowered, a greater portion may be captured by monomer, thus being involved in the polymerization process and increasing the current efficiency.

In the anode compartment of an electrolysis cell, the pH increases if no buffer is present (11). Semiconductor electrodes are sensitive to pH, the flatband voltage shifting 59 mV per change in pH unit (44). Associated with a flat band shift is a shift in the energy of the conduction and valence bands. This is

reflected in the energy of holes from n-type materials. This shift in band energies is analogous to a change in potential of a metal electrode, possibly causing a change in the reactants oxidized. Use of acetic acid with sodium acetate as a supporting electrolyte buffers the solution, minimizing effects due to pH change. The dependence of polymerization on pH was not determined.

Table V

Current efficiencies for various supporting electrolyte systems

Supporting electrolyte	Current Efficiency (moles/faraday)	Relative efficiency
H_2SO_4	63.9	1.40
Na_2SO_4	45.7	1.00
TEAP	55.0	1.20
HOAc - NaOAc	3070.	67.06

III.2.3. Variation in Monomer Concentration

The propagation step of free-radical polymerizations in solution is generally independent of initiation source when

polymerization occurs in the bulk of the solution. For free-radical polymerizations, the rate of polymerization, R_p can be written

$$R_p = \left(\frac{k_p^2}{2k_t} \right)^{0.5} R_i^{0.5} [M] \qquad [49]$$

where k_p is the rate constant for polymerizations, k_t the rate constant for termination and R_i the rate of initiation. The rate of polymerization is defined as the instantaneous decrease of monomer concentration, [M], with respect to time, t, and can be written

$$R_p = \frac{-d[M]}{dt} \qquad [50]$$

Since the rate of polymerization depends on the concentration of monomer, extrapolation to zero time allows the instantaneous rate of polymerization to be determined for the initial concentration of monomer. The rate of polymerization can be determined from the initial slope of a plot of [M] versus t. Such plots are usually sufficiently linear up to 10 to 15% monomer depletion that the slope of a straight line through the first one or two points can be taken as R_p. Polymerizations were conducted in aqueous solutions of 2.0 M acetic acid containing 1.0 M sodium acetate. Monomer concentrations were determined at regular time

intervals from samples withdrawn from the reaction vessel during polymerization. Data scattering on plots of [M] as a function of t was too great to calculate initial rates with any certainty. The data for the polymerization of acrylamide is presented in Table VI. While it was not possible to determine values for R_p, the percentage of the initial concentration of monomer polymerized decreased with decreasing monomer concentrations. The result may be explained in terms of various reactions which compete for the initiating species, methyl radicals, the three main reactions being

a) The radical reacts with a monomer unit initiating a growing polymer chain.

$$CH_3^{\cdot} + M \longrightarrow CH_3M^{\cdot} \qquad [51]$$

b) The radical reacts with a growing polymer chain to terminate growth.

$$CH_3^{\cdot} + R_n^{\cdot} \longrightarrow P_nCH_3 \qquad [52]$$

c) The radical combines with another radical to produce the Photo-Kolbe coupling product.

$$2CH_3^{\cdot} \longrightarrow C_2H_6 \qquad [53]$$

In the absence of monomer, dimerization of methyl radicals by

the anode compartment of divided photoelectrochemical cell using n-TiO_2 electrodes has been demonstrated (19,22). The addition of monomer would result in a competition for the radicals by the two reactions, (a) and (b), as outlined. When the concentration of monomer is decreased and the concentration of methyl radicals kept constant, the probability of a radical reacting with a monomer unit to initiate a growing chain is decreased. As a result, current efficiencies decrease at lower concentrations of monomer. This was evidenced by a decrease in current efficiency by about a factor of 10 as the concentration of monomer was halved. These results are consistent with the decrease in percent yield in Table VI. Tari, Yoshizawa et al. (66) demonstrated, in the electrochemical polymerization of acrylamide using an aqueous solution of acetic acid with potassium acetate, that the amount of ethane produced depends on the concentration of acrylamide.

Table VI

Effect of initial monomer concentration on yields of polyacrylamide

Expt.	$[M]_0$	Charge passed (coulombs)	Polymer Yield (%)
H0	0.281	0.4856	47.3
H1	0.141	0.6686	14.0
H2	0.070	0.5750	2.9
H5	0.000	0.6060	0.0

When the concentration of acrylamide was above 2.4 M, ethane production was negligible. When concentrations were lower than 2.4 M, an increase in ethane production was linked to lower acrylamide concentrations.

When the rate of initiator formation is constant, it would be expected that molecular weights of polymers formed would decrease as concentrations of monomer were decreased. Molecular weight values calculated using intrinsic viscosity data, shown in Table VII, show that a decrease in molecular weights corresponded to decreases in [M]. The decrease in yield and molecular weights corresponding to lower monomer concentrations are consistent with free-radical polymerizations that take place in the bulk of solution.

Table VII

Molecular weight dependence on monomer concentration

Expt.	$[M]_0$	[n] dl/g	M_n	Retention times (min.)
H0	0.281	3.5	420,000	46.8
H1	0.141	3.1	350,000	51.6
H2	0.070	2.9	310,000	54.2

III.2.4. Effect of Light Intensity

Current in electrochemical cells is changed by increasing or decreasing the potential of the electrode. Current in photoelectrochemical cells may be varied by controlling the intensity of light focused on the photoelectrode without appreciably changing the potential of the minority carriers. This can be a significant advantage if increasing the potential of the electrode would promote undesirable side reactions. When the Kolbe electrosynthesis is induced at metal electrodes, the process exhibits a characteristic steady log (current density)/anode potential curve in both aqueous and non-aqueous solvents (99-101). Kolbe dimerization is associated with high anode potentials (ca. 2.4V vs NHE) and the complete suppression of oxygen evolution. In Fig. 13, the lower Tafel slope is associated with evolution of oxygen and the upper slope describes the production of ethane. With use of n-TiO_2 photoanodes, this occurrence of oxygen production should be avoided when current levels are changed by altering the light intensity as the energy of the holes are not affected. Bard et al. have reported the Photo-Kolbe reaction using acetate ions in photoelectrochemical cells equipped with n-TiO_2 photoanodes at several light intensities. Production of methane in one compartment cells and ethane in two compartment cells were reported as the major products.

Kobayashi et al. (88), Gomes et al. (14), and Fujishima,

Figure 13. ANODE POTENTIAL (VS. NHE) AS A FUNCTION OF LOG (CURRENT DENSITY) FOR THE ELECTROLYSIS OF 0.5 M AQUEOUS SODIUM ACETATE (Ref. 99)

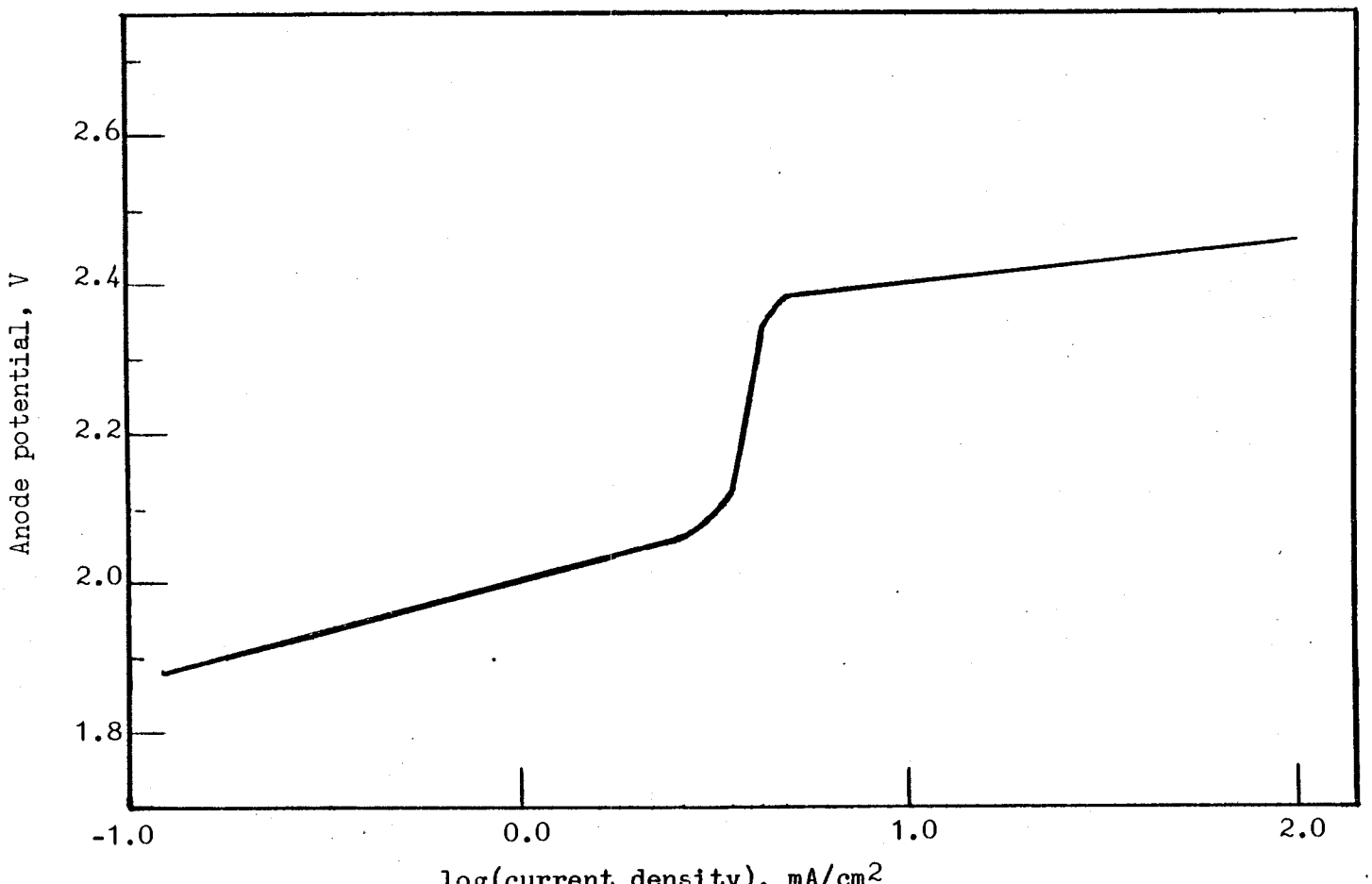
Anode potential, V
2.6
2.4
2.2
2.0
1.8
-1.0
0.0
1.0
2.0
log(current density), mA/cm2

Honda and Inone (87) have reported that the fraction of photocurrent responsible for the oxidation of a species in competition with another species for the holes on n-TiO_2 is independent of light intensity. Therefore, in the competition for n-TiO_2 holes between acetate ions and water, the ratio should remain constant for all intensities of light.

Electrolytic initiation often implies a significant degree of control over the rate of initiation, the rate of polymerization and the molecular weight of the polymer. A significant aspect of this work was to investigate if this control can be accomplished in photoelectrochemical cells by using light intensities to control photo-produced currents. Light intensities were altered by passing the beam of light through neutral density filters before illuminating the photoanode.

The coulometric data for each experiment show that photocurrents remained constant for the duration of the experiments. A plot of coulombs passed vs time is shown in Fig. 14. The linearity of the plot signifies that the rate of oxidation remained constant for the entirety of polymerization and the electrode surface was not coated with an insulating film of polymer.

Polymer yields, calculated as the percent conversion of monomer, for polymerizations of acrylamide at various light intensities are shown in Figs. 15 - 18. Polymerization data is listed in Table VIII. The rates of polymerization were calculated from the change in monomer concentration from t=0 to t=30

Figure 14. PASSAGE OF CHARGE AS A FUNCTION OF TIME FOR ACRYLAMIDE POLYMERIZATION

In aqueous solution of 2.0 M acetic acid - 1.0 M sodium acetate; bias potential 2.000 volts vs SCE.

(a) Light intensity 500 mW/cm^2,

(b) Light intensity 397 mW/cm^2,

(c) Light intensity 158 mW/cm^2,

(d) Light intensity 50 Mw/cm^2.

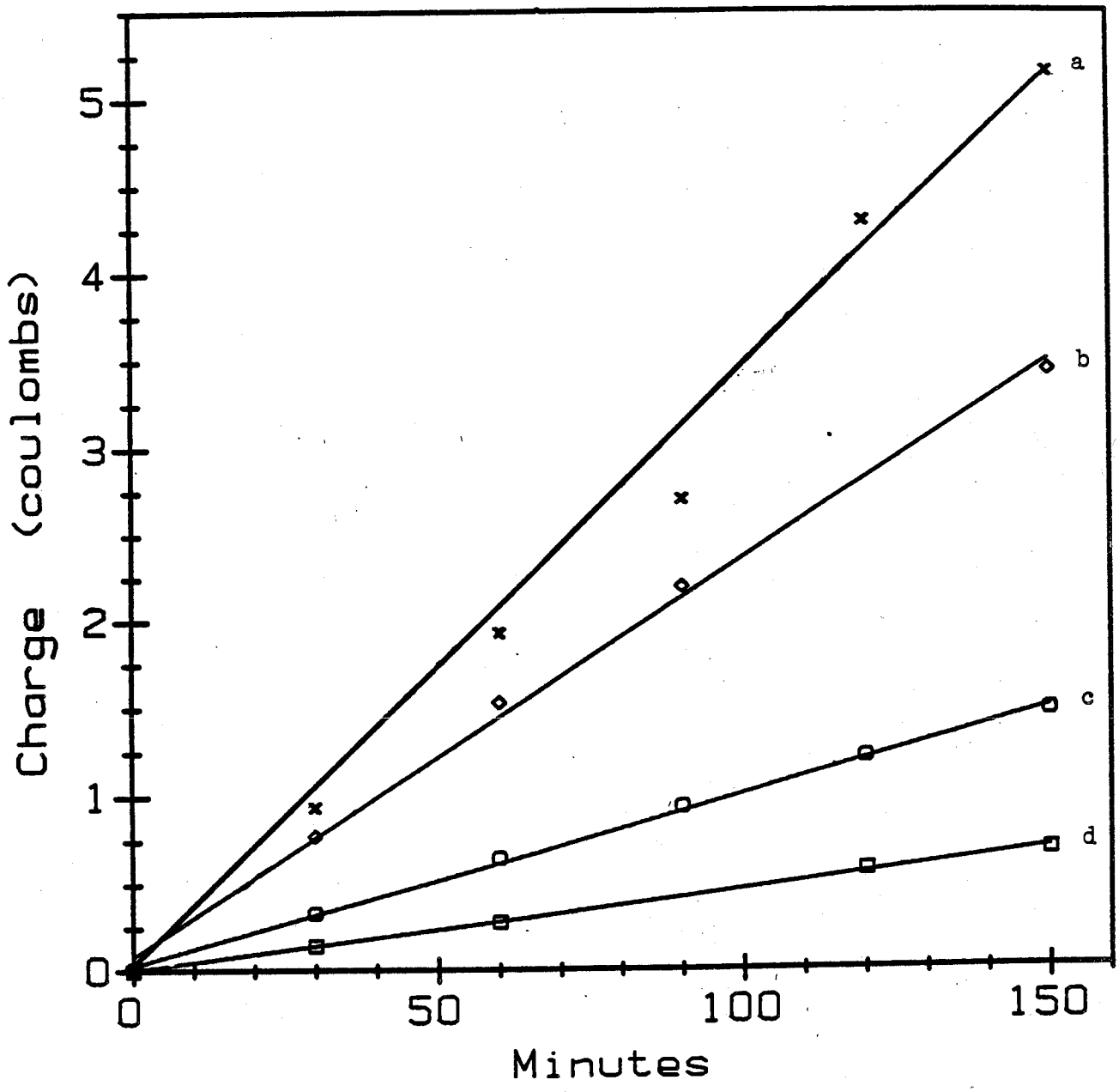
Charge (coulombs)
0
1
2
3
4
5
0
50
100
150
Minutes
a
b
c
d

Figure 15. DEPENDENCE OF POLYACRYLAMIDE YIELD ON THE NUMBER OF COULOMBS PASSED: LIGHT INTENSITY 500 mW/cm^2

In aqueous solution of 2.0 M acetic acid - 1.0 M sodium acetate; bias potential 2.000 volts vs SCE.

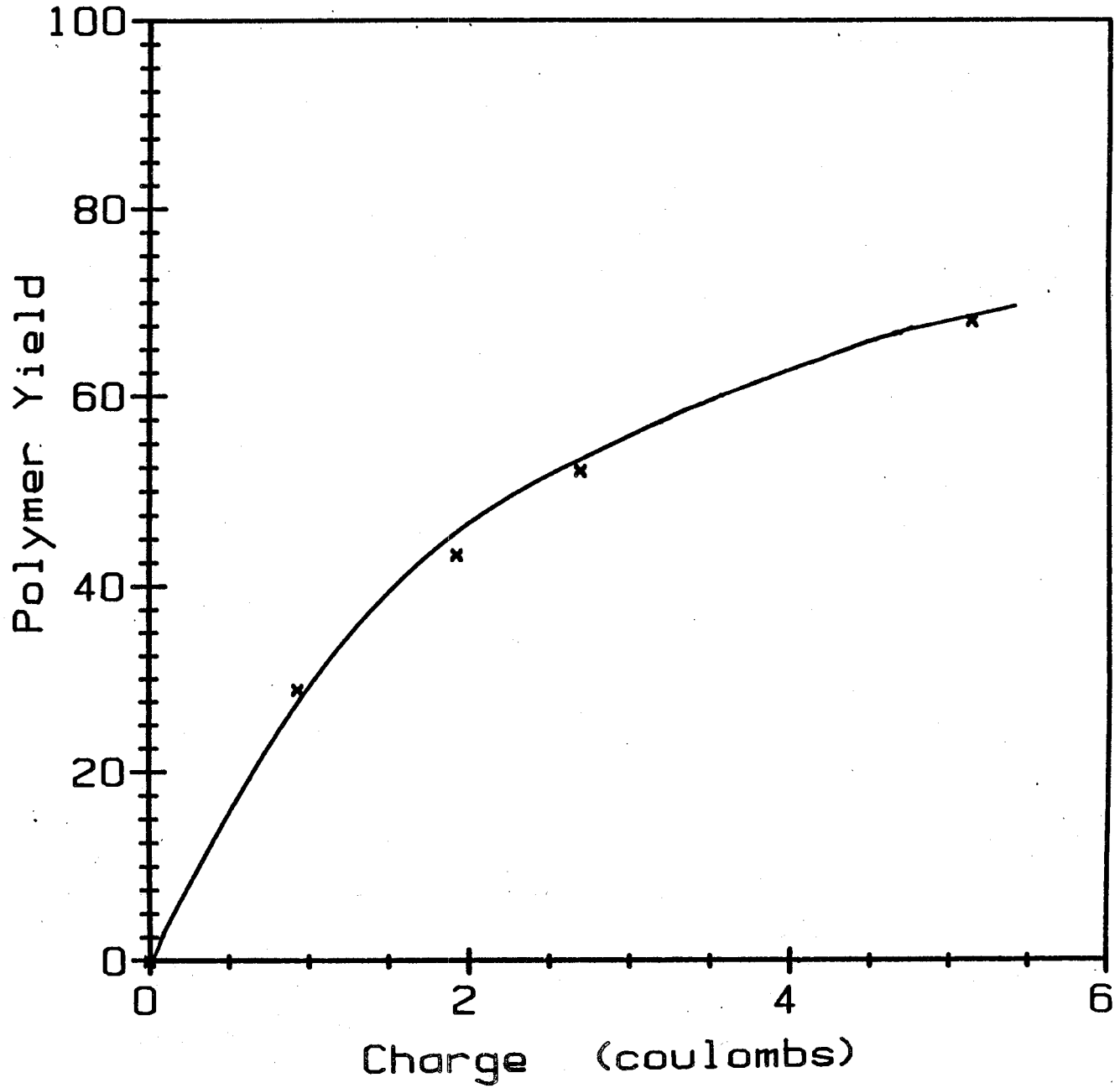
100
80
60
40
20
0
Polymer Yield
0
2
4
6
Charge (coulombs)

Figure 16. DEPENDENCE OF POLYACRYLAMIDE YIELD ON THE NUMBER OF COULOMBS PASSED: LIGHT INTENSITY 397 mW/cm^2

In aqueous solution of 2.0 M acetic acid - 1.0 M sodium acetate; bias potential 2.000 volts vs SCE.

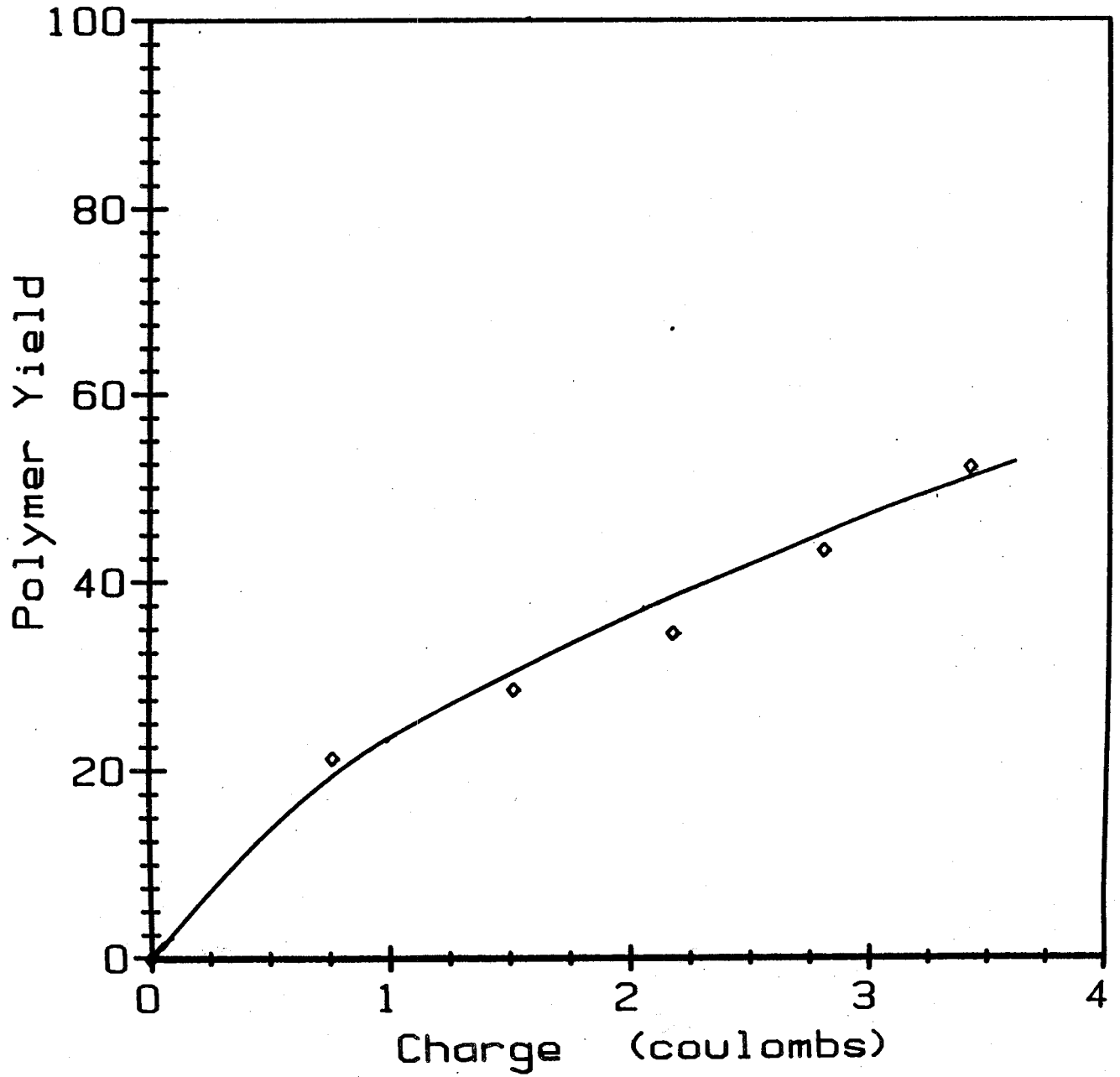
100
80
60
40
20
0
Polymer Yield
0
1
2
3
4
Charge (coulombs)

Figure 17. DEPENDENCE OF POLYACRYLAMIDE YIELD ON THE NUMBER OF COULOMBS PASSED: LIGHT INTENSITY 158 mW/cm^2

In aqueous solution of 2.0 M acetic acid - 1.0 M sodium acetate; bias potential 2.000 volts vs SCE.

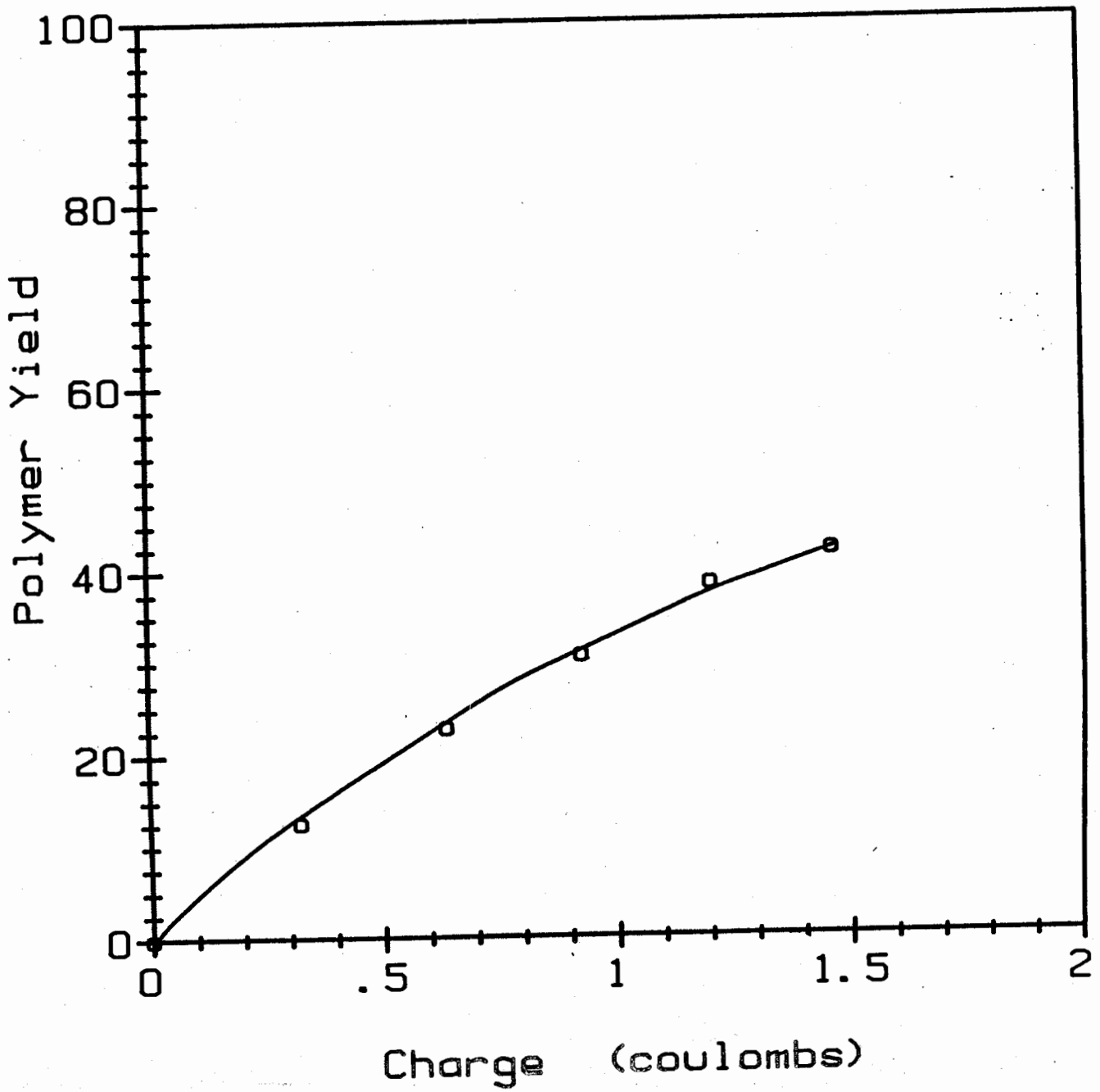
100
80
60
40
20
0
Polymer Yield
0
.5
1
1.5
2
Charge (coulombs)

Figure 18. DEPENDENCE OF POLYACRYLAMIDE YIELD ON THE NUMBER OF COULOMBS PASSED: LIGHT INTENSITY 50 mW/cm^2

In aqueous solution of 2.0 M acetic acid - 1.0 M sodium acetate; bias potential 2.000 volts vs SCE.

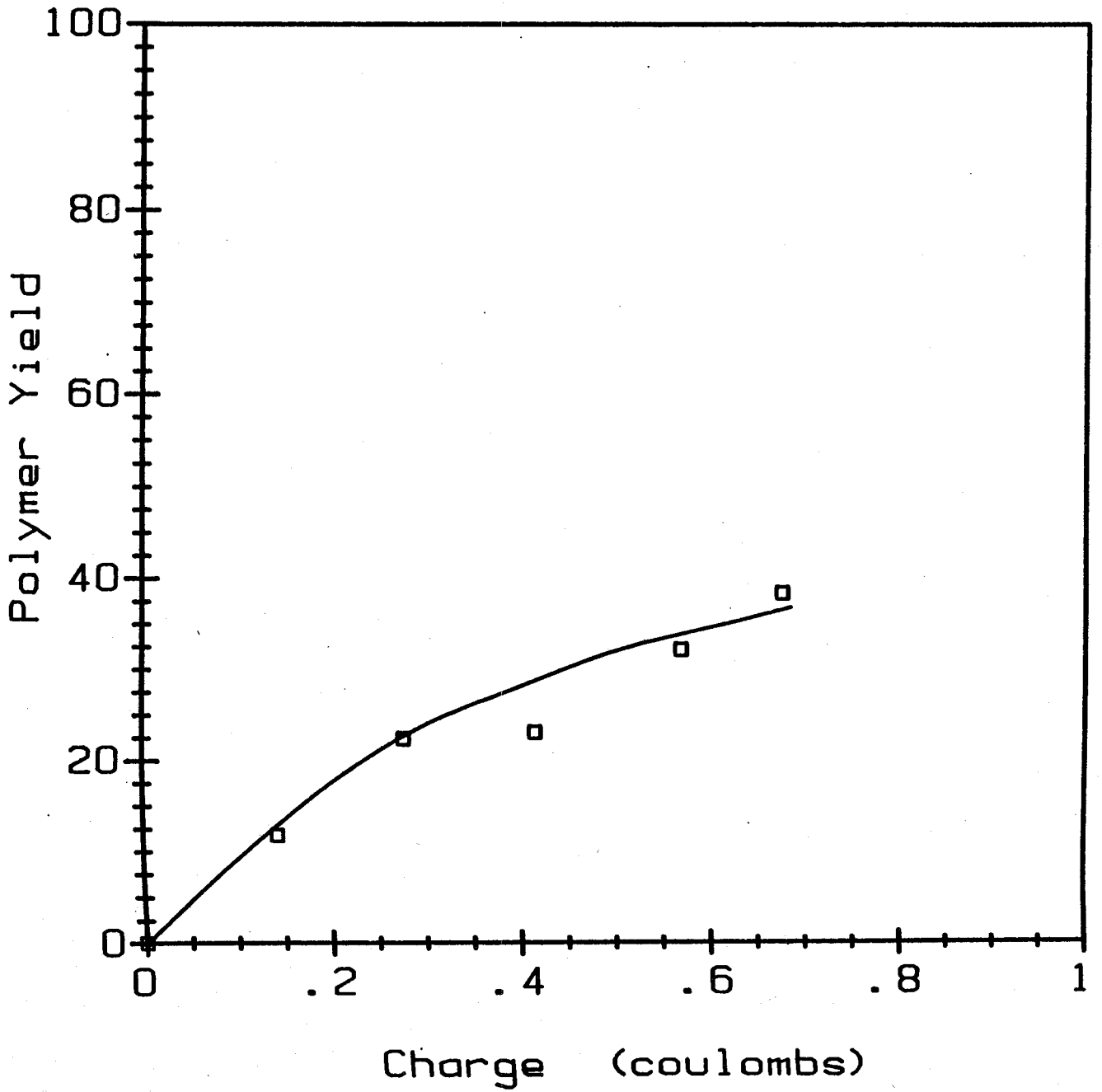
100
80
60
40
20
0
Polymer Yield
0
.2
.4
.6
.8
1
Charge (coulombs)

minutes. R_p values are listed in Table IX. It was observed that R_p values increased with current but no direct empirical relation could be established. In order to establish a relation, it was necessary to take into account the efficiency of initiation, f (6), in terms of the fraction of current involved in the polymerization process.

Values of f were calculated as outlined in the following section on efficiencies. The amount of current involved in polymerization, I*, was calculated

$$I^* = fI \qquad [54]$$

The linearity of the plot of R_p vs I* to the one-half power demonstrates the adherence of the system to the free-radical relation previously shown in equation [49]. At constant initial monomer concentrations, an increase in I* would increase the probability of termination for a growing chain reducing the molecular weight of the polymer. Decreases in I* should have the opposite affect as the lifetime of a growing chain is increased, yielding polymer of higher molecular weight. Starting with the equation

$$\nu = \frac{R_p}{R_i} \qquad [55]$$

Table VIII

Light intensity control of polymer yields

Expt.	Light intensity mW/cm^2	Charge passed (coulombs)	Average current (uA)	Polymer yield (%)
NI	500	5.14	530	67.9
NIV	397	3.42	398	52.2
NV	158	1.46	168	42.0
NIII	50	0.68	77	38.4
Blank	0	0.00	0	0.00

Table IX

Polymerization rates relating to I*

Expt.	R_p (moles/litre-sec)	I* (uA)
NIII	2.7×10^{-5}	7.29
NV	2.9×10^{-5}	9.61
NIV	5.0×10^{-5}	21.16
NI	6.7×10^{-5}	39.69

Figure 19. LINEAR DEPENDENCE OF THE RATE OF POLYMERIZATION ON I^*

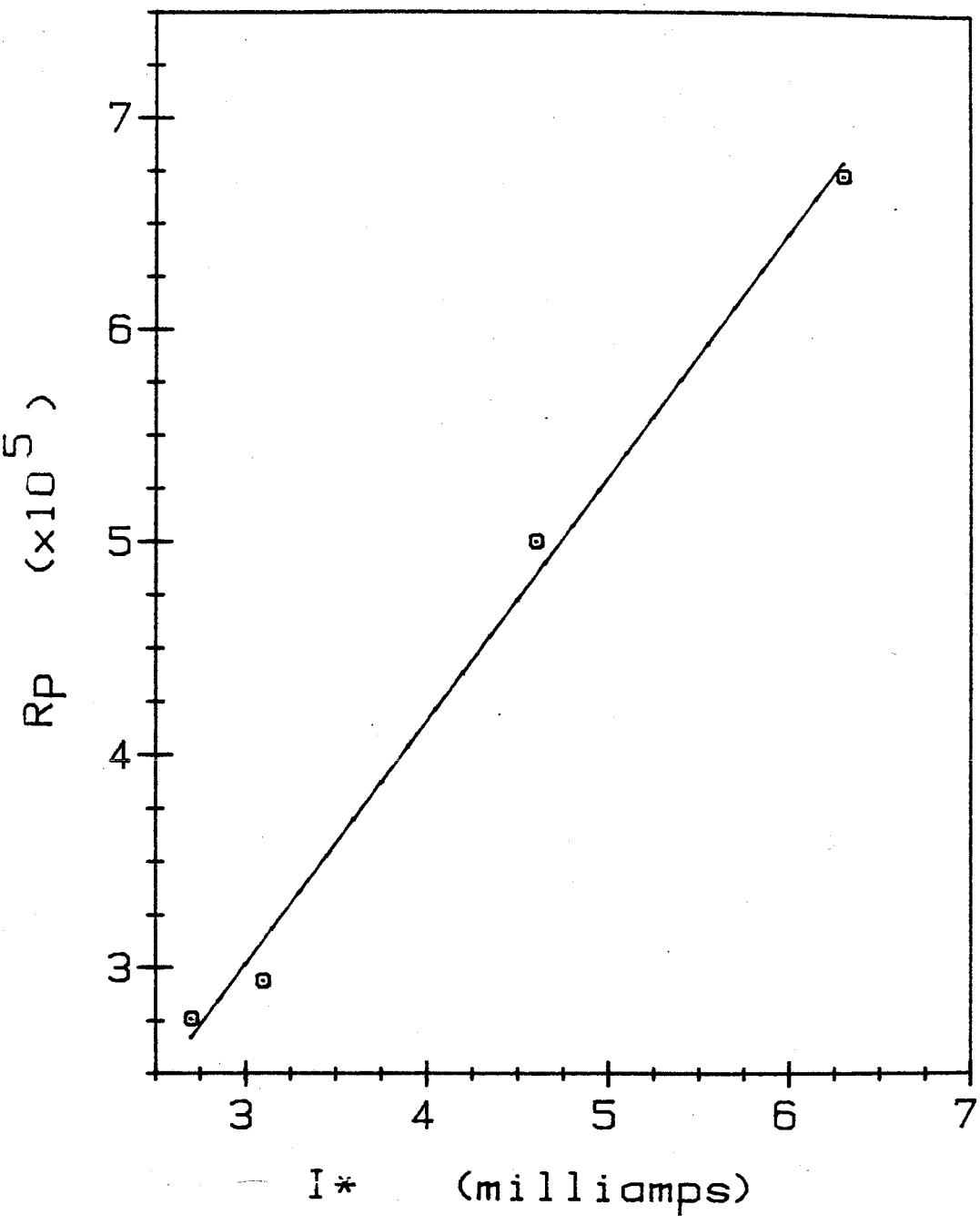
7
6
5
4
3
Rp (x10^5)
3
4
5
6
7
I* (milliamps)

where ν is the average kinetic chain length in radical polymerization, a relation between MW and I^* can be derived. Substituting R_p from equation [49] into equation [55], one gets

$$\nu = \frac{1}{R_i^{0.5}} \left(\frac{k_p^2}{2k_t} \right)^{0.5} [M] \qquad [56]$$

as k_t, k_p and [M] can be regarded as constant,

$$k = \left(\frac{k_p^2}{2k_t} \right)^{0.5} [M] \qquad [57]$$

equation [56] can be simplified to

$$\nu = k \frac{1}{R_i^{0.5}} \qquad [58]$$

If chain transfer is negligible, the molecular weight becomes equal to the kinetic chain length. When initiation is caused by an electrolytic event, the rate of initiation, R_i, is equal to I^* times a constant

$$R_i = k' I^* \qquad [59]$$

Therefore, MW can be substituted into equation [58] for ν and I^* for R_i (where C = a constant)

$$MW = C \frac{1}{I^{*0.5}} \qquad [60]$$

Figure 20. LINEAR DEPENDENCE OF MOLECULAR WEIGHT ON $1/I^{*0.5}$

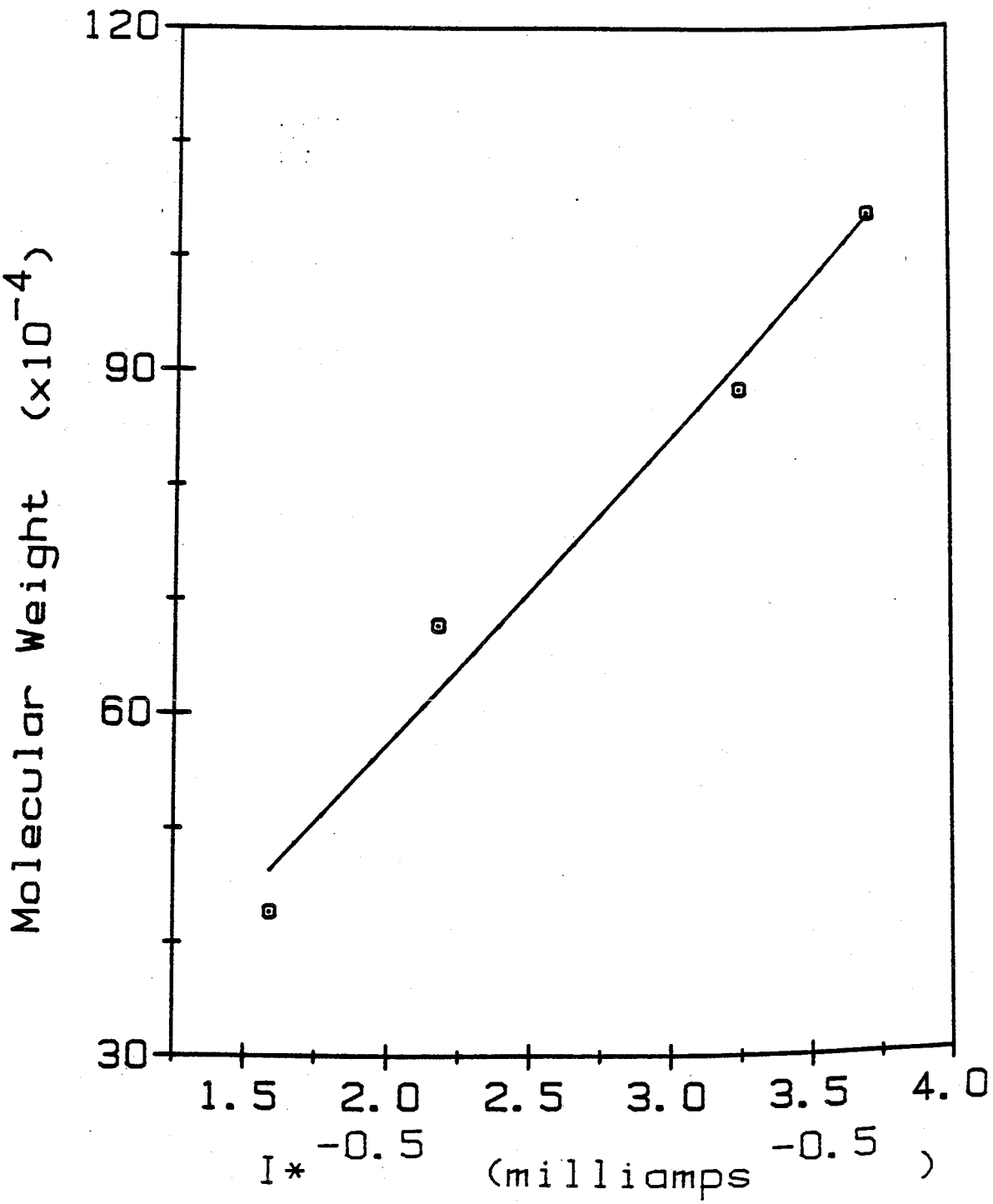
120
90
60
30
Molecular Weight (x10^{-4})
1.5
2.0
2.5
3.0
3.5
4.0
I* $^{-0.5}$ (milliamps $^{-0.5}$)

An increase in molecular weights corresponding to lower current levels was noted as given in Table X. The plot of MW vs the $1/I^{*0.5}$ in Fig. 20, is linear, establishing that the theoretical relation is supported by the experimental results. Molecular weights of polyacrylamide polymerized photoelectrochemically were considerably higher than those reported for Kolbe electrosynthesis (95,97,98,102).

Table X

Molecular weight dependence on light intensity

Expt.	[n] dl/g	M_n	Light intensity (mW/cm^2)
NI	3.5	420,000	500
NIV	4.8	680,000	397
NV	5.7	880,000	158
NIII	6.3	1,030,000	50

III.2.5. Efficiencies

Termination of growing radical chains occurs when the radical end of the chain reacts with another radical. There are typically four ways in which this can take place; a) the polymer radical couples with a primary or initiator radical, b) the polymer radical combines another polymer radical, c) transfer of an atom from one polymer radical to another (disproportionation),

d) by transfer of the radical to another monomer molecule or chain transfer agent.

$$a)\ R_n^{\cdot} + R' \longrightarrow P_nR \qquad [61]$$

$$b)\ R_n^{\cdot} + R_m^{\cdot} \longrightarrow P_{n+m} \qquad [62]$$

$$c)\ R_n^{\cdot} + R_m^{\cdot} \longrightarrow P_n + P_m \qquad [63]$$

$$d)\ R_n^{\cdot} + X \longrightarrow P_n + X^{\cdot} \qquad [64]$$

A theoretical limit for the number of chains formed can be arrived at by dividing the number of electrons passed through the cell by two. Such a limit, based on two electrons per chain, one both for initiation and termination, does not reflect the size of the chains.

$$\text{Theoretical limit} = .5\ (\text{faradays})\ 6.023 \times 10^{23} \qquad [65]$$

The initiation efficiency, f, is defined as the fraction of current, which passes through the cell, that is involved in the polymerization process; f can be calculated

$$f = \frac{\text{number of polymer chains}}{\text{theoretical limit}} \qquad [66]$$

The number of polymer chains produced during polymerization experiment can be calculated using the equation

$$\text{number of polymer chains} = \frac{n \quad 6.023 \times 10^{23}}{\frac{M_n}{\text{MW of monomer}}} \qquad [67]$$

where n is the moles of monomer polymerized. Initiation efficiencies, calculated at the end of polymerization, dropped significantly as initial monomer concentrations were decreased. An increase in ethane production is believed to be associated with the decrease in initiation efficiency. At lower monomer concentrations, the probability that primary radicals will couple rather than initiate or terminate polymerizations increases (103). Initiation efficiencies did not show any appreciable change due to light intensity variation. Table XI lists current efficiencies and initiation efficiencies for polymerizations of acrylamide calculated at the termination of polymerizations. A decrease in current efficiency by a factor of 10 corresponds to a decrease of 2 in monomer concentration. Such a decrease in current efficiency is similar to the decrease in initiation efficiency for the same experiments. An increase in ethane production for lower monomer concentrations would account for both results.

The results also show that current efficiencies increased with lower current passage for similar initial monomer concentrations. The preliminary postulation would be to ascribe the increase in efficiency to a greater fraction of primary radicals being involved in the polymerization process. However, the values of initiation efficiencies do not support the

postulation. In order for the increase in current efficiency to be caused by a greater fraction of primary radicals participating in polymerization, it would be necessary that the initiation efficiency increase as well. As this did not occur, the increase in current efficiency must be attributed to a different phenomena. The following explanation may account for the increase

Table XI

Current efficiencies and initiation efficiencies for acrylamide polymerizations

Expt.	[M]	Polymer yield (%)	Faradays ($\times 10^6$)	Current efficiency	Initiation efficiency (f)
H0	0.281	47.3	5.0	2640	0.865
H1	0.141	14.0	6.9	285	0.113
H2	0.070	2.9	6.0	34	0.016
NI	0.281	67.9	53.3	537	0.076
NIV	0.281	52.2	34.5	622	0.053
NV	0.281	42.2	15.1	1170	0.056
NIII	0.281	38.4	7.1	2300	0.098

in current efficiency. Lower currents passing through the cell result in lower rates of primary radical production. This is reflected in increased lifetimes of the average growing polymer chain as lowering of the concentration of primary radicals reduces the probability of primary radical termination. The

longer lifetimes of the growing chain would lead to increases in molecular weights, an effect established earlier. Consequently, for lower currents, an increased number of moles of monomer are polymerized per faraday, increasing the current efficiency without affecting the initiation efficiency.

It was noted that both initiation and current efficiencies decrease with an increase in the time of polymerization. In Table XII are listed the current efficiencies calculated for various instances during the course of polymerization. The marked decrease in efficiency is attributed to a constant rate of oxidation coinciding with a decrease in monomer concentration. As photoelectrolysis continues, an increasing portion of current is involved in producing non-polymeric products. It is presumed that the decreases in current and initiation efficiencies, with respect to polymer production, would be associated with an increase in both efficiencies with respect to ethane production.

Table XII

Current efficiencies as a function of sampling times

Expt.	30 min.	60 min.	90 min.	120 min.	150 min.
NI	1270	970	789	617	538
NIV	1131	768	646	575	621
NV	1582	1457	1348	1209	1172
NIII	3351	3286	--	2301	2308

III.3. Polymerization of Ethyl Vinyl and Isobutyl Vinyl Ethers

III.3.1. Polymerization in Acetonitrile

The ultraviolet spectra of solutions of 0.10 M tetraethylammonium perchlorate in acetonitrile containing ethyl vinyl ether and isobutyl vinyl ether showed that no absorbance occurred at wavelengths longer than 200 nm. Since the Hg lamp used for a light source had essentially no emissions below 200 nm, it was concluded that no photopolymerization of either monomer would interfere during attempts to initiate their polymerization photoelectrochemically. Under experimental conditions, this was verified as no polymerization of either monomer occurred when solutions of acetonitrile and tetraethylammonium perchlorate containing the individual monomers were illuminated with unfiltered light from the Hg lamp for durations up to 30 minutes. No electroinitiation of either monomer occurred when solutions containing monomer were in contact with a TiO_2 electrode held at a potential of 2.000 volts vs SCE as long as the cell was kept in dark conditions. However, onset of polymerization began when the biased photoelectrode was illuminated with light of energy greater than the 3.0 eV band gap energy of TiO_2.

During polymerization of ethyl vinyl ether, the solution developed a brownish-yellow coloration which deepened with an increase in passage of current. The constant level of current

during the entirety of the reaction is evidenced by the linearity of Fig. 21. Monomer conversion as a function of charge passed is shown in Fig. 22. The resulting polymers were viscous, sticky liquids with the consistency of heavy oil. Poly(ethyl vinyl ether) retained the same brownish-yellow coloration that had developed in solution during polymerization. The infrared spectrum of the polymer is shown in Fig. 23.

No coloration of solution was associated with the polymerization of isobutyl vinyl ether in solutions of acetonitrile containing tetraethylammonium perchlorate. While the polymer of isobutyl vinyl ether had the same consistency as that of poly(ethyl vinyl ether), poly(isobutyl vinyl ether) was clear and colorless. The data reported in Table XIII illustrates the results of the ethyl vinyl ether polymerization and Table XIV the results of isobutyl vinyl ether polymerization in acetonitrile at various temperatures. It was observed that poly(isobutyl vinyl ether) precipitated onto the photoelectrode, reducing the area of the electrode exposed to solution. The decrease in current, indicated by the non-linearity of Fig. 25, is believed to be caused by the precipitation of the polymer onto the electrode. The infrared spectrum of poly(isobutyl vinyl ether) produced photoelectrochemically is shown in Fig. 24.

Figure 21. PASSAGE OF CHARGE AS A FUNCTION OF TIME FOR ETHYL VINYL ETHER POLYMERIZATION

Supporting electrolyte TEAP; bias potential 2.000 volts vs SCE.

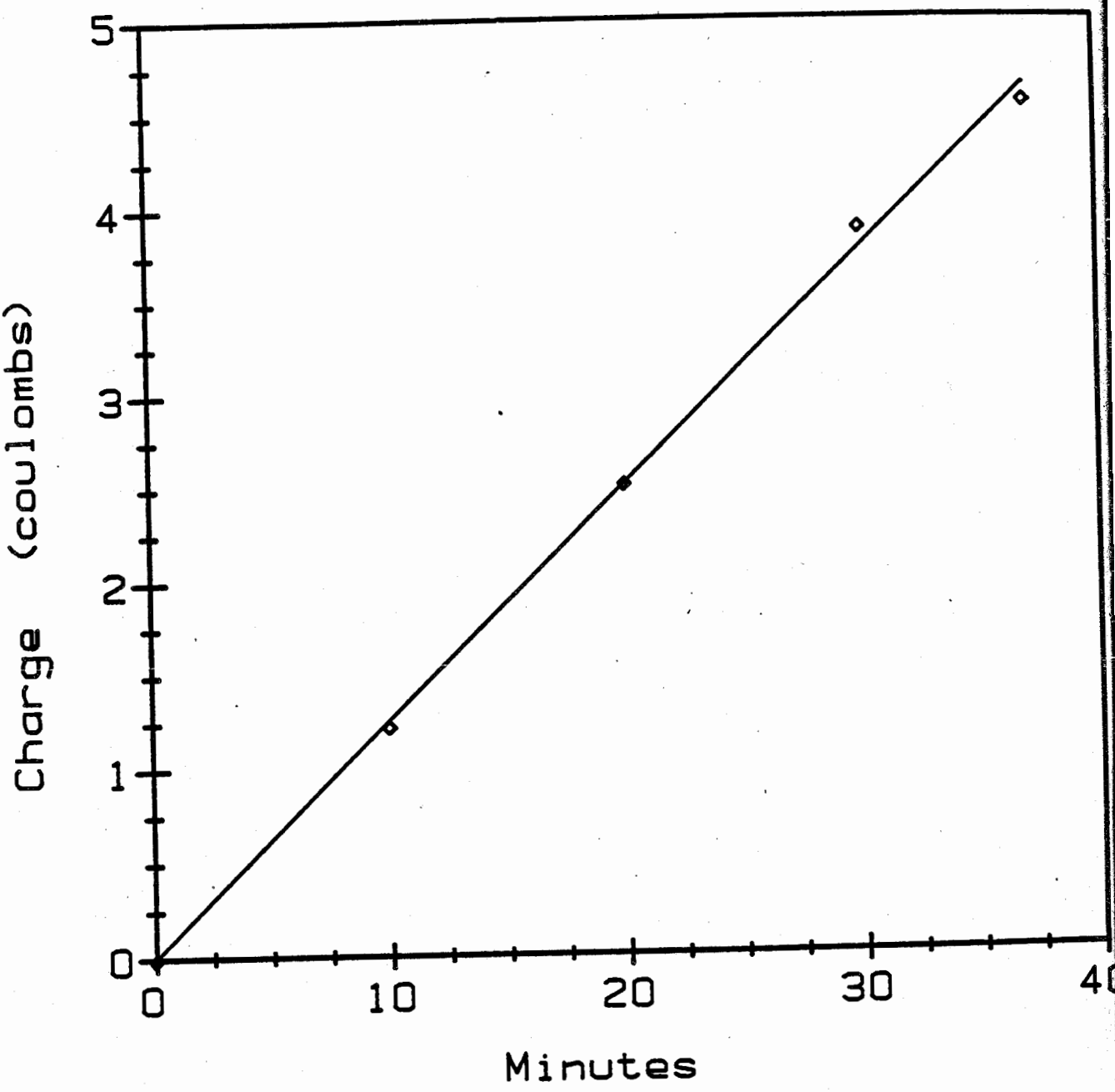
Charge (coulombs)
5
4
3
2
1
0
0
10
20
30
Minutes

Figure 22. DEPENDENCE OF YIELD OF POLY(ETHYL VINYL ETHER) ON THE NUMBER OF COULOMBS PASSED

In solution of 0.10 M TEAP in acetonitrile; bias potential 2.000 volts vs SCE.

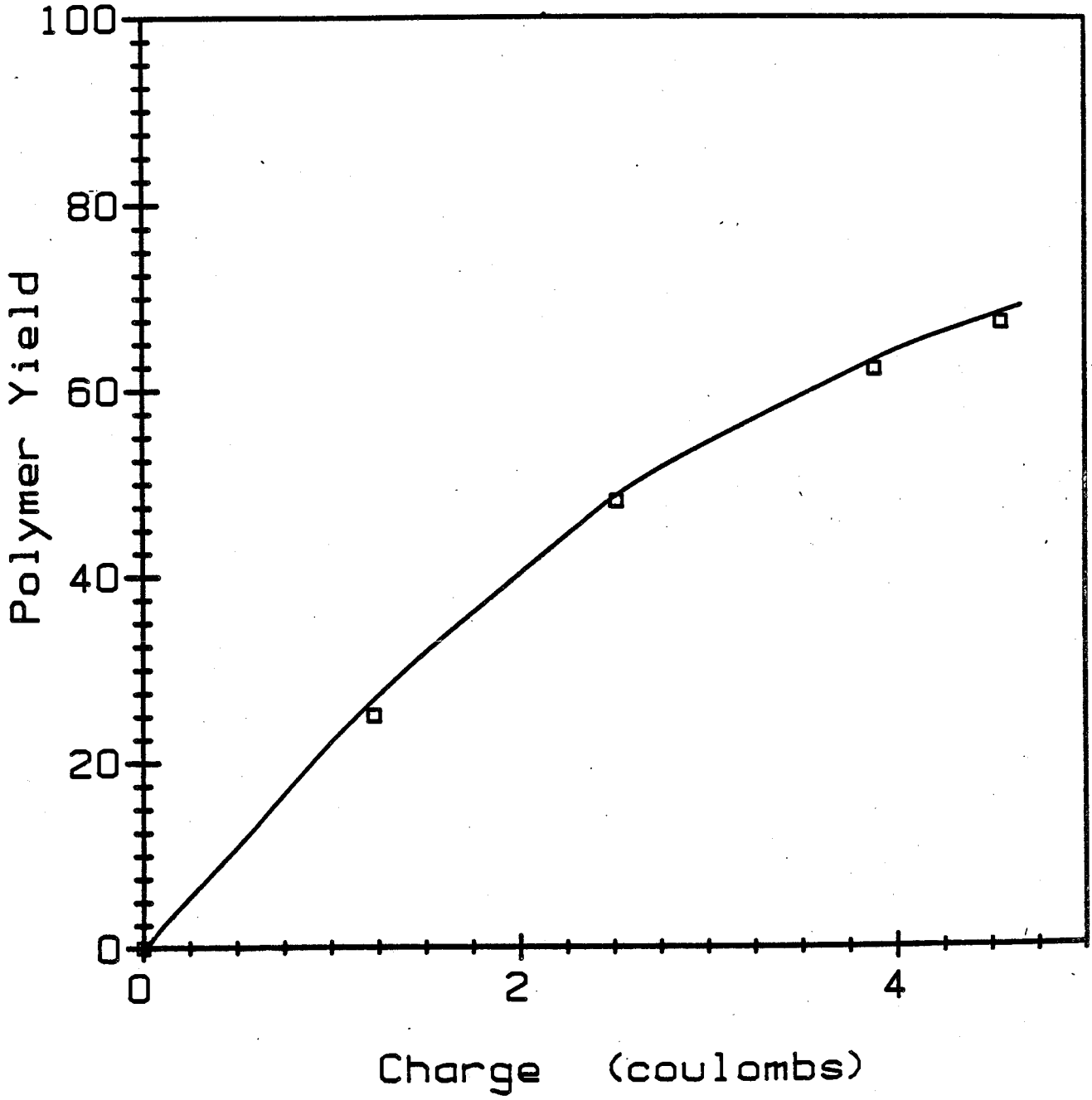
100
80
60
40
20
0
Polymer Yield
0
2
4
Charge (coulombs)

Figure 23. INFRARED SPECTRUM OF POLY(ETHYL VINYL ETHER)

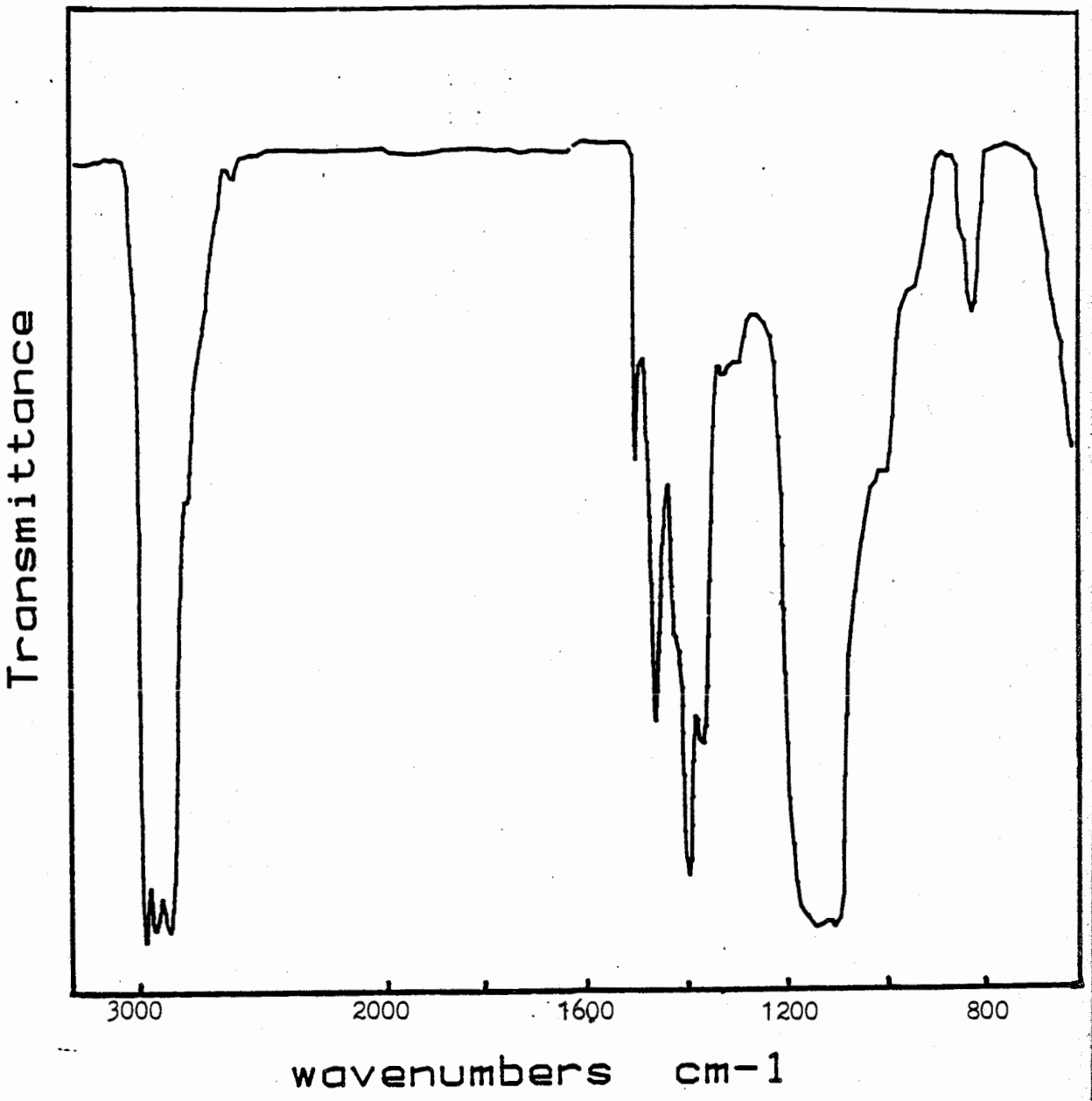
Transmittance
3000
2000
1600
1200
800
wavenumbers cm-1

Figure 24. INFRARED SPECTRUM OF POLY(ISOBUTYL VINYL ETHER)

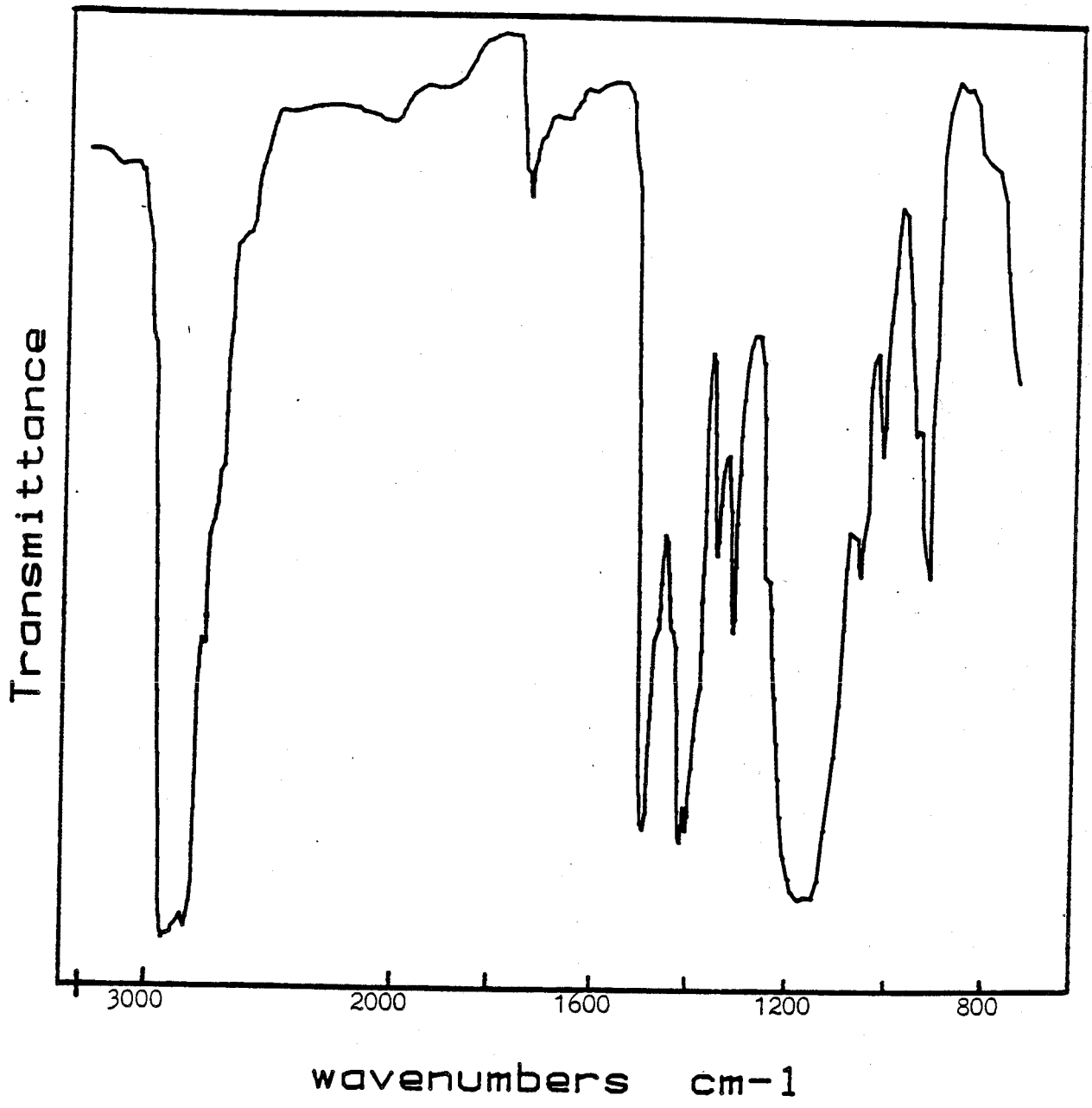
Transmittance
3000
2000
1600
1200
800
wavenumbers cm-1

Figure 25. PASSAGE OF CHARGE AS A FUNCTION OF TIME FOR THE POLYMERIZATION OF ISOBUTYL VINYL ETHER IN ACETONITRILE

(a) temperature = 10 °C
(b) temperature = 0 °C

Supporting electrolyte TEAP; bias potential 2.000 volts vs SCE.

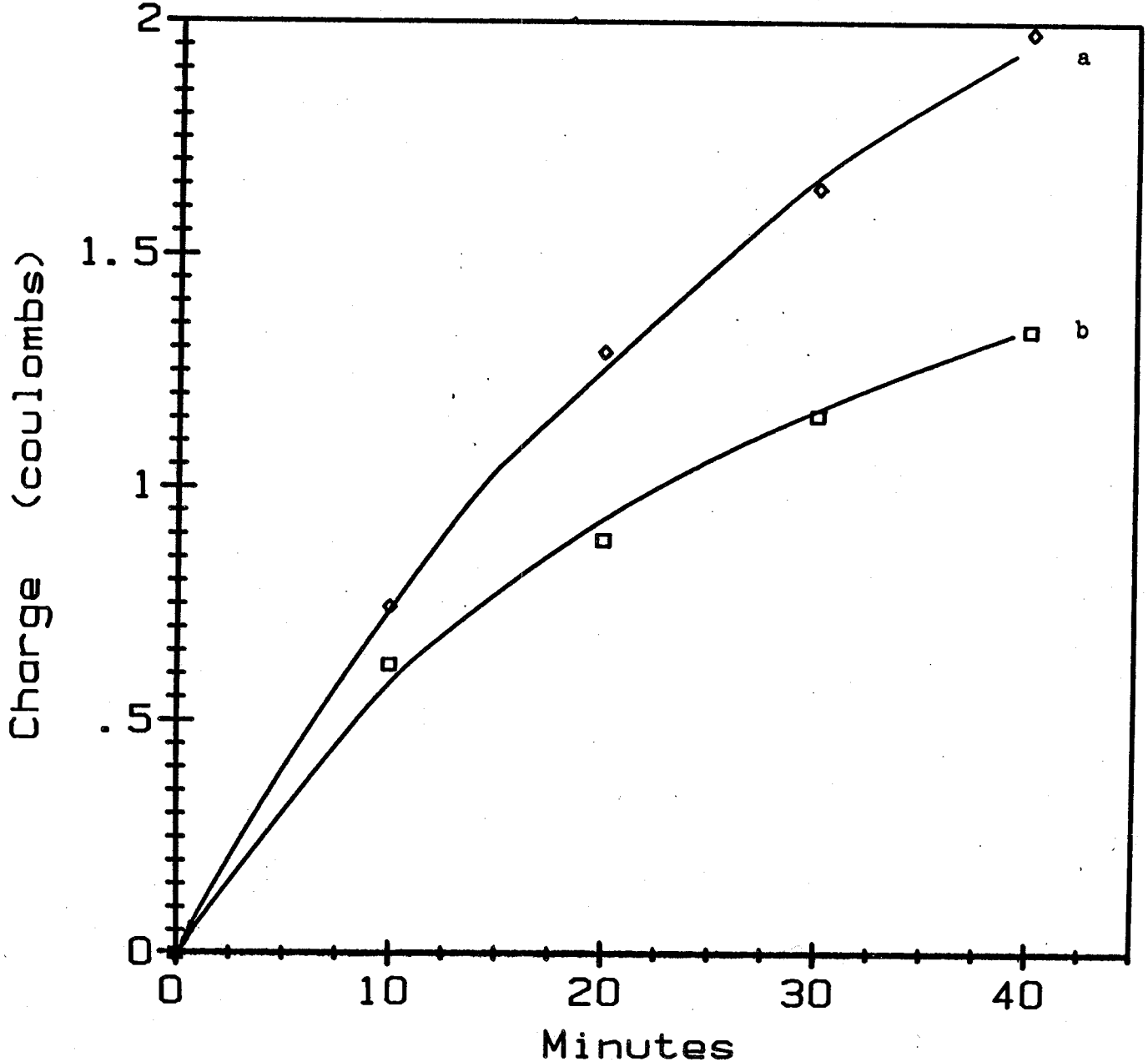
2
1.5
1
.5
0
Charge (coulombs)
0
10
20
30
40
Minutes
a
b

Poly(vinyl ethers) prepared from homogeneously initiated polymerizations, generally have low molecular weights, which are normally attributed to the high value of transfer constants to monomer in these polymerizations. Typical values for molecular weight of poly(ethyl vinyl ether) and poly(isobutyl vinyl ether) polymerized electrochemically are in the range of 2000 to 15,000 (103-106). Polymers of poly(ethyl vinyl ether) and poly(isobutyl vinyl ether) produced photoelectrochemially in acetonitrile have molecular weights as shown in Table XV. Molecules of both poly(ethyl vinyl ether) and poly(isobutyl vinyl ether) polymerized in acetonitrile would more accurately be termed oligomers as molecular weights are below 1000 and the degree of

Table XIII

Effect of charge passed on the polymerization of ethyl vinyl ether

Temperature (°C)	Charge passed (coulombs)	Polymer yield (%)
-10	1.224	25
	2.510	48
	3.877	62
	4.548	67
-17	4.076	81
-25	1.792	75
	3.402	92

polymerizations below 10. The low values of molecular weights can not be completely attributed to the high rates of transfer rate to monomer. In addition, transfer to or termination by a species not removed from the solvent or supporting electrolyte during purification or created by a photoelectrochemial event would have to occur to explain the low molecular weights.

Table XIV

Effect of charge passed on the poylmerization of isobutyl vinyl ether in acetonitrile

Temperature (°C)	Charge passed (coulombs)	Polymer yield (%)
10	0.744	15
	1.290	18
	1.641	22
	1.978	23
0	0.621	10
	0.889	14
	1.156	16
	1.339	17

A partial or total independence of current with respect to monomer concentration is suggested by the decrease of current efficiency with the passage of current. With a metal electrode,

this result could be taken as an indication that direct electron transfer between the electrode and monomer does not take place. The mechanism for electron transfers at semiconductor electrodes is still a matter of much investigation but may involve a

Table XV

Influence of polymerization temperature on molecular weights of vinyl ethers in acetonitrile

Monomer	Temperature (°C)	M_n	M_w	M_w/M_n
EVE	- 10	360	420	1.16
EVE	- 17	690	850	1.24
EVE	- 25	510	570	1.12
IBVE	10	700	800	1.17
IBVE	0	830	1000	1.23

competitive process between several species in solution. As such, it is not possible from the data secured to determine the mechanism by which the vinyl ethers were initiated.

There are two alternative means by which the initiation of cationic polymerizations of vinyl ether may occur. They can be divided into the two following categories

a) polymerization proceeds with direct photoelectrochemical initiation where transfer of electrons take place directly from a

monomer unit to the electrode to generate active centers;

b) polymerization proceeds with indirect photoelectrochemical initiation where the transfer of electrons occur between the electrode and any of the substrates present in the solution, except monomer, bringing about the formation of catalytic species which in turn are capable of initiating polymerization.

If initiation were to proceed only by direct transfer to monomer, current would be expected to be dependent on monomer concentration. The exception would be the case where oxidation of monomer occurred in competition with the oxidation of another species in solution which was not involved in the initiation of polymerization. In such a case, the fraction of current oxidizing each species would change as the concentration of monomer decreased so as to keep the current constant.

Evidence for the indirect electrochemical initiation of many cationic polymerizations through the anodic oxidation of the supporting electrolyte or other added species has been cited in literature (106-112). The two species present in solution which could be oxidized to cause the indirect initiation are the solvent and perchlorate ion from the supporting electrolyte. It was presumed that the perchlorate anion of tetraethylammonium perchlorate would be preferentially oxidized rather than the acetonitrile solvent. Proposed mechanisms, based on a

Table XVI

Current efficiencies for the polymerization of vinyl ethers in acetonitrile

Monomer	Temperature (°C)	Faradays ($x10^6$)	Current efficiency
EVE	-10	12.7	890
		26.0	842
		40.2	697
		47.5	636
IBVE	10	7.7	636
		13.4	456
		17.0	429
		20.5	371
IBVE	0	6.4	482
		9.2	478
		12.0	426
		13.9	389

perchlorate radical initiation of ethyl vinyl ether or isobutyl vinyl ether would follow one of the following routes

a) Hydrogen extraction from a species in solution to produce perchloric acid followed by H^+ initiation

$$ClO_4^{\cdot} + HX \longrightarrow HClO_4 + X^{\cdot} \quad [68]$$

$$HClO_4 + CH_2{=}CHOR \longrightarrow [HCH_2\text{-}CHOR]^+ + ClO_4^- \quad [69]$$

b) Oxidation of monomer

$$ClO_4^{\cdot} + CH_2{=}CHOR \longrightarrow ClO_4^- + [CH_2\text{-}CHOR]^{+\cdot} \quad [70]$$

Through indirect initiation, perchlorate concentrations would remain essentially constant during the course of polymerization allowing current to remain constant. As a result, current levels would remain independent of monomer concentration and current efficiencies would drop with time as products other than polymer were formed through the process of photoelectrolysis.

III.3.2. Polymerization of Isobutyl Vinyl Ether in Dichloromethane

Polymerization of isobutyl vinyl ether in dichloromethane was attempted at three light intensities. Due to the low solubility of tetraethylammonium perchlorate in dichloromethane, tetrabutylammonium perchlorate was used as a supporting electrolyte. While dichloromethane is considered to be a better solvent for cationic polymerizations than acetonitrile, the solution conductivity of dichloromethane is considerably lower than that of acetonitrile. For this reason, dichloromethane was not considered an ideal choice as a solvent in which to conduct photoelectrochemical experiments.

Polymerizations were conducted at 0 °C with a bias of 3.000

volts vs SCE applied to the semiconductor electrode. Solutions of isobutyl vinyl ether in dichloromethane did not polymerize photochemically nor did they polymerize electrochemically when in contact with an electrode bias of 3.000 volts under dark conditions. Monomer conversion was determined to have exceeded 85% for each experiment when photoelectrosynthesis was terminated after 20 minutes. Poly(isobutyl vinyl ether) produced in dichloromethane was a colorless, sticky, semi-solid. The data for molecular weights of poly(isobutyl vinyl ether) polymerized in dichloromethane for several light intensities are listed in Table XVII.

Table XVII

Influence of light intensity on molecular weights of poly(isobutyl vinyl ether) in dichloromethane

Relative light intensity	Initial current	M_n	M_w	M_w/M_n
8	1.91 mA	5,800	16,000	2.76
4	1.00 mA	6,300	12,000	1.84
1	0.25 mA	9,800	20,000	2.04

IV. CONCLUSION

The work reported here constitutes the first radical polymerization of acrylamide and cationic polymerization of vinyl ethers initiated by a photoelectrochemical event. It was demonstrated that no additional sources acted as initiators for polymerization. Polymerizations were initiated in the anode compartment of a divided photoelectrochemical cell using a single crystal n-TiO_2 electrode as a photoanode.

In general, all holes produced through light absorbed by n-type semiconductors reach the electrode/solution interface with the same potential. As the rate at which holes are produced dictates the anodic process, current levels can be controlled through variations in light intensity at the photoelectrode. Photoelectrochemical initiated polymerizations are unique in that the rates of initiation can be controlled through variations in current levels without changing the working potential of the photoanode. Initiation by a photoelectrochemical current provided a degree of control over the polymerization of acrylamide. An increase in the amount of current passed resulted in an increase in the rate of polymerization and decrease in molecular weights. A decrease in initial monomer concentration at constant current resulted in a decrease in polymer yield and molecular weights.

An investigation of the kinetics of acrylamide polymerization showed that the rate of polymerization was one-half order with respect to the portion of current participating in the polymerization process I*. It was further

demonstrated that molecular weights were related to the inverse of I* to the one-half power.

Current efficiencies were greatest when an acetic acid and sodium acetate supporting electrolyte system was used for free radical polymerizations. The large affinity of acetate ions for the holes of n-TiO_2 was suggested to be responsible for the greater current efficiencies than those of other supporting electrolytes. Values in the range of 5 to 10 % were obtained for current efficiencies with acetate ions. A decrease in efficiency with time was demonstrated with respect to polymer production. Presumably, an increase in efficiency with respect to ethane production accompanied the decrease.

The work here encompasses the first polymerization of a vinyl ether initiated by a photoelectrochemical technique. The mechanism of polymerization of the vinyl ethers is believed to be cationic. Production of oligomers in acetonitrile and low polymers in dichloromethane was accomplished. Several possible mechanisms for the electron transfer between the anode and species in solution which subsequently initiated polymerizations were discussed.

V. LIST OF REFERENCES

1. H. R. Allcock, F. W. Lampe: Contemporary Polymer Chemistry, Prentice-Hall, Inc., New Jersey (1981).
2. F. W. Billmeyer Jr.: Textbook of Polymer Science, Wiley-Interscience, N. Y. (1976).
3. A. Ledwith: Pur. Appl. Chem., 49, 431 (1977).
4. G. Oster, N. Yang: Chem Revs., 68, 125 (1968).
5. H. Shirota, H. Mikawa: Macromol. Sci., C16(2), 129 (1978).
6. G. Odian: Principles of Polymerization, Wiley-Interscienc, N.Y. (1981).
7. G. Silvestri, S. Gambino, G. Filardo: Adv. Polymer Sci., 38, 27 (1981).
8. N. Yamasaki: Adv. Polymer Sci., 6, 377 (1969).
9. P. Giusti: J. Polym. Sci. Symp. No. 50., 133 (1975).
10. B. L. Funt: Macromol. Revs., 1, 35 (1966).
11. S. N. Bhadani, G. Parranao, in "Organic Electrochemisty", M. M. Baizer, and H. Lund, Eds., Marcel Dekker, Inc., N. Y. (1983).
12. B. L. Funt, in "Macromolecular Review", Vol. 1, Interscience, N. Y. (1962).
13. A. Fujishima, K. Honda: J. Chem. Soc. Japan, 44, 1148 (1971).
14. F. Vanden Kerchove, A. Praet, W. P. Gomes: J. Electrochem. Soc., 132, 2357 (1985).

15. E. Borgarello, J. Kiwi, M. Gratzel, E. Pelizzetti, M. Visca: J. Am. Chem. Soc., 104, 2996 (1982).

16. T. Inoue, T. Watanabe, A. Fujishima, K. Honda: Chemistry Letters, 1073 (1977).

17. S. Sato J. M. White: J. Phys. Chem., 85, 336 (1981).

18. S. Sato, J. M. White: J. Am. Chem. Soc., 102, 7206, (1980).

19. B. Kraeutler, A. J. Bard: J. Am. Chem. Soc., 93, 7729 (1977).

20. B. Kraeutler, A. J. Bard: J. Am. Chem. Soc., 100, 2239 (1978).

21. H. Yoneyama, Y. Takao, H. Tamura A. J. Bard: J. Phys. Chem., 86, 1417 (1983).

22. B. Kraeutler, A. J. Bard: J. Am. Chem. Soc., 100, 5985 (1978).

23. H. Miyama, N. Fujii, Y. Nagae: Chem. Phys. Lett., 74, 523 (1980).

24. M. A. Fox, M. Chen: J. Am. Chem Soc., 105, 4497 (1983).

25. J. A. Switzer, E. L. Moorehead, D. M. Dalesandio, J. Electrochem. Soc., 129, 2232 (1982).

26. A. J. Bard, J. Photochemistry, 10, 59 (1979).

27. A. J. Bard, J. Electroanal. Chem., 168, 5 (1984).

28. H. Gerischer, Int. Union Pure App. Chem. 29th,; Chem. For Future Proc., H. Gruewald Ed., 11 (1983).

29. A.S.Lakshmanam, C. V. Suryanarayana: SAEST, 18, 281 (1983).

30. A. J. Nozik: Ann. Rev. Chem., 29, 189 (1978).

31. K. Rajeshwar: J. App. Electrochem., 15, 1 (1985).

32. M. S. Wrighton in "Inorganic Chemistry; Towards the 21st Century", ACS Symp. Series 211, M. H. Chisholm Ed., (1983).

33. M. S. Wrighton: Pure Appl. Chem., 57, 57 (1985).

34. S. R. Morrison: The Chemical Physics of Surfaces, Plenum Press, New York (1977).

35. A. J. Bard: J. Phys. Chem., 86, 172 (1982).

36. M. A. Fox: Acc. Chem. Res., 16, 314 (1983).

37. H. Gerischer in "Topics in Applied Physics", vol 31, B. O. Seraphin Ed., Springer-Verlag, Berlin-Heidelberg-New York (1977).

38. H. Gerisher in "Advances in Electrochemistry and Electrochemical Engineering", vol 1, P. Delahay Ed., Interscience (1961).

39. H. Gerisher in "Physical Chemistry", vol 1XA, H. Eyring, D. Henderson, W. Jost, Eds., Academic Press, New York (1970).

40. T. Freund, W. P. Gomes: Catal. Rev., 3, 1 (1969).

41. A. J. Bard, L. R. Faulkner in "Electrochemical Methods: Fundamentals and Applications", Wiley, New York (1980).

42. G. Nagasubramanian, B. L. Wheeler, A. J. Bard: J. Electrochem. Soc., 130, 1680 (1983).

43. R. Memming: J. Electrochem. Soc., 125, 117 (1978).

44. S. R. Morrison: Electrochemistry at Semiconductor and Oxidized Metal Electrodes, Plenum Press, New York (1980).

45. A. H. A. Tinnemans, T. P. M. Koster, D. H. M. W. Thewissen, A. Mackor, Comm. Eur. Communit., [Rep]. EUR. 9529, 106 (1984).

46. H. Gerischer: J. Electrochem. Soc., 125, 218C (1978).

47. H. Gerischer: J. Electrochem. Soc., 113, 1174 (1966).

48. K. Rajeshwar, P. Singh and J. DuBow: Electrochimica Acta, 23, 1117 (1978).

49. H. Gerischer: J. Electroanol. Chem. Interfacial Electrochem., 58, 263 (1975).

50. M. S. Wrighton, A. B. Ellis, P. T. Wolczanski, D. L. Morse, H. B. Abrahamson, D. S. Ginley: J. Am. Chem. Soc., 98, 2774 (1976).

51. A. Fujishima, K. Honda: Nature, 283, 37 (1972).

52. C. Stalder, J. Augustynski: J. Electrochem. Soc., 126, 2007 (1979).

53. M. Halmann: Nature, London, 275, 115 (1978).

54. D. Canfield, K. W. Frese Jr.: J. Electrochem. Soc., 130, 1772 (1983).

55. B. Aurian-Blajeni, M. Halmann, J. Manassen: Sol. Energy. Mat., 8, 425 (1983).

56. S. N. Frank, A. J. Bard: J. Am. Chem. Soc. 99, 4667 (1977).

57. F. R. Fan, R. G. Keil, A. J. Bard: J. Am. Chem. Soc., 105, 220, (1983).

58. A. Fujishima, T. Iooru, K. Honda: J. Chem. Soc., 101, 5582 (1979).

59. S. N. Frank, A. J. Bard: J. Am. Chem. Soc., 99, 4667 (1977).

60. E. C. Dutoit, F. Cardon, W. P. Gomes: Berichte der Bunsen-Gesellschaft, 80, 475, (1976).

61. P. R. Harvey, R. Rudham, S. Ward: J. Chem. Soc., Faraday Trns. 1, 79, 1381 (1983).

62. B. Kraeutler, H. Reiche, A. J. Bard: J. Polym. Sci. Polym. Lett. Ed., 17, 535 (1979).

63. B. L. Funt, S. J. Tan: J. Polym. Chem. Ed., 22,605 (1984).

64. P. V. Kamat, R. Basheer, M. A. Fox: Macromol. 18, 1366 (1985).

65. M. Okano, K. Itoh, A. Fujishima, K. Honda: Chem. Lett., 4, 469, (1986).

66. M. E. Gerstner: J. Electrochem. Soc., 126, 944 (1979).

67. A. Praet, F. V. Kerchove, W. P. Gomes, F. Cardon: Solar Energy Materials 7, 481 (1983).

68. F. Liou, C. Y. Yang, S. N. Levine: J. Electrochem. Soc., 130, 893 (1983).

69. R. Noufi, A. J. Frank, A. J. Nozik: J. Am. Chem. Soc., 103, 1849 (1981).

70. S. Menezes, A. Heller, B. Miller: J. Electrochem. Soc., 127, 1268 (1980).

71. N. Yamazaki: Adv. Polym. Sci., 6, 377 (1969).

72. S. N. Bhadani, Y. K. Prasad: Makromol. Chem., 178, 1841 (1977).

73. A. Rudin, R. A. Wagner: J. Appl. Polym. Sci., 19, 3361 (1975).

74. Polymer Handbook, J. Brandrup, E. H. Immergut eds., Interscience, (1967).

75. F. F. Fan, B. Reichman, A. J. Bard: J. Am. Chem. Soc., 102, 1488 (1980).

76. J. O. Bockris, M. Szklarczyk, A. Q. Contractor, S. U. M. Khan: Int. J. Hydrogen Energy, 9, 741 (1984).

77. F. DiQuarto, A. J. Bard: J. Electroanal. Chem., 127, 43 (1981).

78. J. L. Sculfort, D. Guyomard, M. Herlem: Electrochimica Acta, 29, 459 (1984).

79. M. T. Spitler, M. Calvin: J. Chem. Phys., 66, 4294 (1977).

80. J. Moser, M. Gratzel: J. Am. Chem. Soc., 105, 6547 (1983).

81. R. W. Matthews: Aust. J. Chem., 36, 191 (1983).

82. R. H. Wilson, L. A. Harris, M. E. Gerstner: J. Eletrochem. Soc., 126, 844 (1979).

83. D. W. DeBerry, A. Viehbeck: J. Am. Chem. Soc. Comm., 130, 249 (1983).

84. M. A. Malati, W. K. Wong: Surface Technology, 22, 305 (1984).

85. A. J. Noziak: Nature, 257, 383 (1975).

86. J. G. Mauroides, D. I. Tchernev, A. J. Kafalas, D. F. Kolesar: Mat. Res. Bull., 10, 1023 (1975).

87. A. Fujishima, T. Inove, K. Honda: J. Am. Chem. Soc., 101, 5582 (1979).

88. T. Kobayashi, H. Yoneyama, H. Tamura: J. Electroanal. Chem., 122, 133 (1981).

89. K. Hirano, A. J. Bard: J. Electrochem. Soc., 127, 1056 (1980).

90. B. L. Funt, J. Tanner in "Techniques of Electro-organic Synthesis", vol 5, part II, N. L. Weinberg, ed., John Wiley and Sons, New York (1975).

91. A. Gandini, H. Cheradame: Adv. Polym. Sci., 34135 (1980).

92. B. L. Funt, K. C. Yu: J. Polym. Sci., 54, 107 (1961).

93. S. R. Palit: J. Polym. Sci., Pt. C., 31, 241 (1971).

94. S. Yoshizawa, Z. Takehara, Z. Ogymi, C. Nagai: J. Appl. Electrochem., 6, 147 (1976).

95. P. K. Sengupta, R. Chakraborty: J. Macromol. Sci.-Chem., A21, 701 (1984).

96. S. Yoshizawa, I. Tari, M. Suhara: Denki Kagaku, 40, 650 (1972).

97. Z. Ogumi, I. Tari, Z. Takehara, S. Yoshizawa: Bull. Chem. Soc. Jpn., 47, 1843 (1974).

98. Z. Ogumi, I. Tari, Z. Takehara, S. Yoshizawa: Bull. Chem. Soc. Jpn., 49, 841 (1976).

99. L. Eberson, J. H. P. Utley in Organic Electrochemistry M. M. Baizer and H. Lund, eds., Marcel Dekker, Inc., New York, New York (1983).

100. T. F. Otero: Makromol. Chem., Rapid Commun., 5, 125, (1984).

101. A. J. Bard: Science 207, 139 (1980).

102. S. Yoshizawa, I. Tari, M. Suhara, Denki Kagaku, 40, 650 (1972).

103. T. Takahashi, Y. Hori, I. Sato: Bull. Polym. Sci. (A-1), 6, 2091 (1968).

104. D. D. Eley, A. W. Richards: Trans. Farad. Soc., 45, 425 (1962).

105. J. P. Kennedy: J. Polym. Sci., 38, 263 (1959).

106. G. Mengoli, G. Vidotto: Makromol. Chemie, 153, 57 (1972).

107. G. Mengoli, G. Vidotto: Eur. Polymer J., 8, 671 (1972).

108. G. Mengoli, G. Vidotto: Makromol. Chemie, 139, 293 (1970).

109. P. Cerrai, P. Giusti, G. Guerra, M. Tricoli: Eur. Polymer J., 11, 101 (1975).

110. J. P. Billion: J. Electroanal. Chem., 1, 486 (1960).

111. B. L. Funt, T. J. Blain: J. Polm. Sci. (A-1), 8, 3339, (1970).

112. J. W. Breitenbach, F. Sommer, G. Unger: Monatsch. Chem., 107, 359 (1976).